

California AHMCT Program  
University of California, Davis  
California Department of Transportation

## **Vision-based Low Cost Field Demonstrable Paint Restriping Guidance System**

David C. Slaughter, Nelson Smith, Chris Gliever,  
Garrett Jones, and Justin Schlottman

Biological and Ag. Engineering  
University of California, Davis

AHMCT Research Report  
UCD-ARR-01-09-14-02

Final Report for Contract  
RTA 65A0041

February 2002

This work was supported by the New Technology and Research Program of the California Department of Transportation (Caltrans) and the Advanced Highway Maintenance and Construction Technology (AHMCT) Center at the University of California, Davis.

**Technical Report Documentation Page**

1. Report No.	2. Government Accession No.	3. Recipient's Catalog No.	
4. Title and Subtitle  VISION-BASED LOW COST FIELD DEMONSTRABLE PAINT RESTRIPING GUIDANCE SYSTEM		5. Report Date February 2002	6. Performing Organization Code
		8. Performing Organization Report No. UCD-ARR-01-09-14-02	
7. Author(s) David C. Slaughter, Nelson Smith, Chris Gliever, Garrett Jones, and Justin Schlottman		10. Work Unit No. (TRAIS)	
9. Performing Organization Name and Address Biological and Ag. Engineering University of California, Davis Davis, CA 95616		11. Contract or Grant No. RTA 65A0041	
		13. Type of Report and Period Covered Final Report 4/99 to 9/01	
12. Sponsoring Agency Name and Address California Department of Transportation New Technology and Research, MS-83 Sacramento, CA 94372-0001		14. Sponsoring Agency Code	
		15. Supplementary Notes	
16. Abstract  This report describes a developmental feasibility study for the automatic guidance of a lane restriping system to automatically apply paint on top of worn traffic lane boundary striping with a lateral tolerance of +/-13mm and a longitudinal tolerance of +/-102mm for dashed lane striping. This system would assist the California Department of Transportation in their effort to enhance safety, reduce worker stress, improve restriping efficiency, and reduce traffic flow impacts of striping maintenance. Machine vision recognition systems employing both hardware and software based neural network lane stripe recognition were evaluated. Preliminary results show potential for automatic machine vision location of worn traffic lane boundary striping, however additional study is needed to fully evaluate the accuracy of this system. A non-contact radar displacement sensor was found to be an acceptable alternative to a traditional ground-driven encoded wheel sensor for longitudinal control of dash length.			
17. Key Words Lane Striping, Machine Vision, Automatic Guidance, Displacement Sensing, Radar.		18. Distribution Statement No restrictions. This document is available to the public through the National Technical Information Service, Springfield, VA 22161	
20. Security Classif. (of this report) Unclassified	20. Security Classif. (of this page) Unclassified	21. No. of Pages 55	22. Price

## TABLE OF CONTENTS

	<u>PAGE</u>
TECHNICAL REPORT DOCUMENTATION (DOT-F-1700.7)	i
LIST OF FIGURES	iii
LIST OF TABLES	iv
DISCLOSURE STATEMENT	v
DISCLAIMER STATEMENT	v
ACKNOWLEDGEMENT	vi
INTRODUCTION	1
OBJECTIVE	3
OUTRIGGER LATERAL POSITION CONTROL SYSTEM	3
PRINCIPAL OF ZICAM OPERATION FOR LATERAL OUTRIGGER GUIDANCE	8
SYSTEM RESPONSE REQUIREMENTS FOR LATERAL OUTRIGGER GUIDANCE	12
ZICAM DEVELOPMENT CHRONOLOGY AND PERFORMANCE EVALUATION	15
DASH LENGTH CONTROL SYSTEM	18
OPERATOR INTERFACE	21
CONCLUSIONS AND RECOMMENDATIONS	22
APPENDIX A – CAD DRAWINGS FOR ZICAM ENCLOSURE	23
APPENDIX B – ZICAM MANUAL	33
APPENDIX C – RADAR SENSOR SPECIFIICATIONS	44
APPENDIX D – COST BENEFIT ANALYSIS	52
APPENDIX E – CD-ROM MOVIE OF ZICAM OPERATION	55

## LIST OF FIGURES

	<u>PAGE</u>
Figure 1. Caltrans District 10 lane restriping vehicle.	1
Figure 2. Caltrans lane restriping operator adjusting restriping controls while leaning out vehicle window to observe striping performance.	2
Figure 3. Diagram of lateral position control system for the lane restriping outrigger.	4
Figure 4. Machine vision system mounted inside the white enclosure attached to the edgeline outrigger on the starboard side of the striping vehicle with the outrigger in the normal operating position	5
Figure 5. Machine vision system mounted inside the white enclosure attached to the centerline outrigger on the port side of the striping vehicle with the outrigger in the retracted (non-operating) position for storage or high-speed transport.	6
Figure 6. Enclosure interior showing the configuration of the two Zicam machine vision systems.	7
Figure 7. View from the rear operator's window showing the port outrigger in operation and shadows caused by trees adjacent to the roadway.	7
Figure 8. An example of a Radial basis function mapping, where (P1, P2) is stored knowledge from prior training and (V1, V2) is a new visual input to be classified by the network.	9
Figure 9. A raw image of a worn edgeline collected from the Zicam is shown in (a), the image in (b) is the result of averaging columns of pixels from (a) to reduce the intensity variation in (a) due to wear and cracks, the graph in (d) is the vertical profile of the intensity in a column from (c), the red line in (b) is the estimated center of the lane stripe using the vertical profile from (d).	10
Figure 10. Spectral reflectance curves for fresh white and yellow paint and worn asphalt.	11
Figure 11. Typical spectral sensitivity of a monochrome CCD video camera.	11
Figure 12. Visual Basic program interface used to determine the relative position error of the outrigger when operated without the automatic guidance system.	13
Figure 13. Lateral position error of the outrigger when the striping vehicle was operated by an inexperienced driver without the aid of the guidance mirror seen in figure 1. An error of zero indicates that the paint nozzle is located directly above the center of the lane stripe.	14
Figure 14. Power spectral density of the outrigger position when the striping vehicle was operated by an inexperienced driver without the aid of the guidance mirror.	15

Continued on page iv

## LIST OF FIGURES CONTINUED

	<u>PAGE</u>
Figure 15. Step test response of starboard outrigger, valve offset = 2083, proportional gain =8.	16
Figure 16. Step test of starboard outrigger showing the effect of changes in proportional and derivative gain levels.	17
Figure 17. Software interface for automatic recognition of worn lane stripes developed by UC Davis for a standard industrial machine vision computer without the use of the ZISC hardware.	18
Figure 18. Striping vehicle conducting a test of the longitudinal accuracy of dash line length.	19
Figure 19. Redesigned operator interface, showing traditional paint valve switches and a new touch screen display.	21

## LIST OF TABLES

Table 1. Precision of longitudinal control of dash and space lengths.	21
---	----

## DISCLOSURE STATEMENT

The California Department of Transportation and the FHWA reserve a royalty-free, non-exclusive and irrevocable license to reproduce, publish or otherwise use, and to authorize others to use, this work for government purposes.

## DISCLAIMER STATEMENT

The research reported herein was performed as part of the Advanced Highway Maintenance and Construction Technology (AHMCT) Program, at the University of California, Davis and the New Technology and Research Program of the California Department of Transportation.

The contents of this report reflect the views of the author(s) who is (are) responsible for the facts and the accuracy of the data presented herein. The contents do not necessarily reflect the official views or policies of the STATE OF CALIFORNIA or the FEDERAL HIGHWAY ADMINISTRATION or the UNIVERSITY OF CALIFORNIA. This report does not constitute a standard, specification, or regulation.

## ACKNOWLEDGEMENT

The authors would like to express their appreciation for the cooperation provided by George Byrd, and the striping personnel in District 10. Without their invaluable assistance this research study would not have been possible.

## INTRODUCTION

Each year the California Department of Transportation expends about 58 person-years and \$7.5 million (including labor costs)<sup>1</sup> in its highway maintenance program for the striping of 67,000 stripe miles (107,826 km) on California roadways. This report describes a research project conducted to assess the feasibility of developing a vision-based low cost field demonstrable paint restriping guidance system and a radar displacement sensor to assist Caltrans in their effort to enhance safety, reduce worker stress, improve restriping efficiency, and reduce traffic flow impacts of traffic lane striping maintenance.

The majority of the striping task is conducted with a lane striping vehicle similar to that shown in figure 1. The lane striping vehicle requires two operators, one to drive the vehicle, and another in the rear to operate the paint controls. In addition to the normal driving tasks, the driver uses a mirror (shown mounted to the extended bar in front of the vehicle in figure 1) to carefully guide



Figure 1. Caltrans District 10 lane restriping vehicle.

---

<sup>1</sup> Caltrans Striping Quality Improvement Committee. 2000. Final Report on the state of statewide maintenance striping operations. December.

the vehicle so that the paint nozzle(s) (mounted on an extendable arm called an outrigger at the mid portion of the vehicle) are accurately positioned over the existing lane stripe to be repainted.

Striping is typically conducted at a travel speed of 32 kph (20 mph), requiring great concentration from highly skilled striping operators. In its current implementation, the task is tedious, fatiguing, and forces the operators to work in non-optimal positions while attempting to accurately and precisely control the application of traffic lane striping. For example, figure 2 shows the rear striping operator leaning his head out the vehicle window in order to observe the striping operation while simultaneously reaching in the opposite direction in order to adjust a paint control knob. This scene is typical of the working environment of the striping operation and has a direct impact upon safety, the quality of the traffic lane striping and the level of operator stress.



Figure 2. Caltrans lane restriping operator adjusting restriping controls while leaning out vehicle window to observe striping performance.

The restriping operation requires a lateral (perpendicular to the direction of travel) accuracy of  $\pm 13$  mm ( $\pm 0.5$  inches) and a longitudinal (in the direction of travel) accuracy (for dashed lane markings) of  $\pm 102$  mm ( $\pm 4$  inches). At the normal travel speed of 32 kph, a slight hesitation by the operator in excess of one eighty-eighth of a second (0.0114 seconds) when changing striping patterns will cause the pattern transition to miss its intended location by a distance in excess of 102 mm. In many cases, particularly with less experienced or fatigued operators, the

driver must significantly reduce the vehicle speed when approaching a pattern transition in order to accommodate the skill level of the operator and maintain quality control standards. Further, slight differences in the accuracy of the vehicle displacement sensors of different striping vehicles in a district results in an accumulated error when repainting dashed lines and forces the rear striping operator to constantly readjust the dash and skip lengths, significantly increasing the difficulty of the task. In the current implementation, restriping safety and accuracy are inversely correlated with productivity.

## OBJECTIVE

The goal of this project was the development of low-cost field demonstrable guidance systems for paint restriping to assist Caltrans in their effort to enhance safety, reduce worker stress, improve restriping efficiency, and reduce traffic flow impacts. The project sought to develop a low-cost real-time machine vision sensor for lateral guidance and to adapt a low-cost radar displacement sensor for longitudinal guidance in paint restriping operations. The project was designed to include a potential manufacturer as a cooperator from the start of the project in an effort to reduce the time from development to deployment. General Vision (formerly Neuroptics, Petaluma, CA) was selected as the cooperating manufacturer because of its ZISC neural network image processing technology and low-cost (approximately \$5,000) compact, intelligent camera technology (Zicam), and because General Vision president, Guy Paillet, had prior experience with the development of an autonomous, unmanned, hazard warning vehicle which followed the edge of the lane using a machine vision sensor.

## OUTRIGGER LATERAL POSITION CONTROL SYSTEM

The automatic control system for lateral position control of the lane restriping outrigger is shown in figure 3. Each lane restriping outrigger is actuated by a hydraulic cylinder. To control the lateral position of the outrigger a position sensor (model JX-PA50-N11-111-321, Unimeasure, Corvallis, OR) was attached in parallel to each of the outrigger's hydraulic cylinders. The position sensor was interfaced to a microcontroller (model BirdBox, Tern Inc., Davis, CA) and the microcontroller was interfaced to the existing proportional directional hydraulic control valve (model D1P0133421211011A5 871058 026 27244, Denison Hydraulics UK Ltd.) which controlled the hydraulic flow to the cylinders.

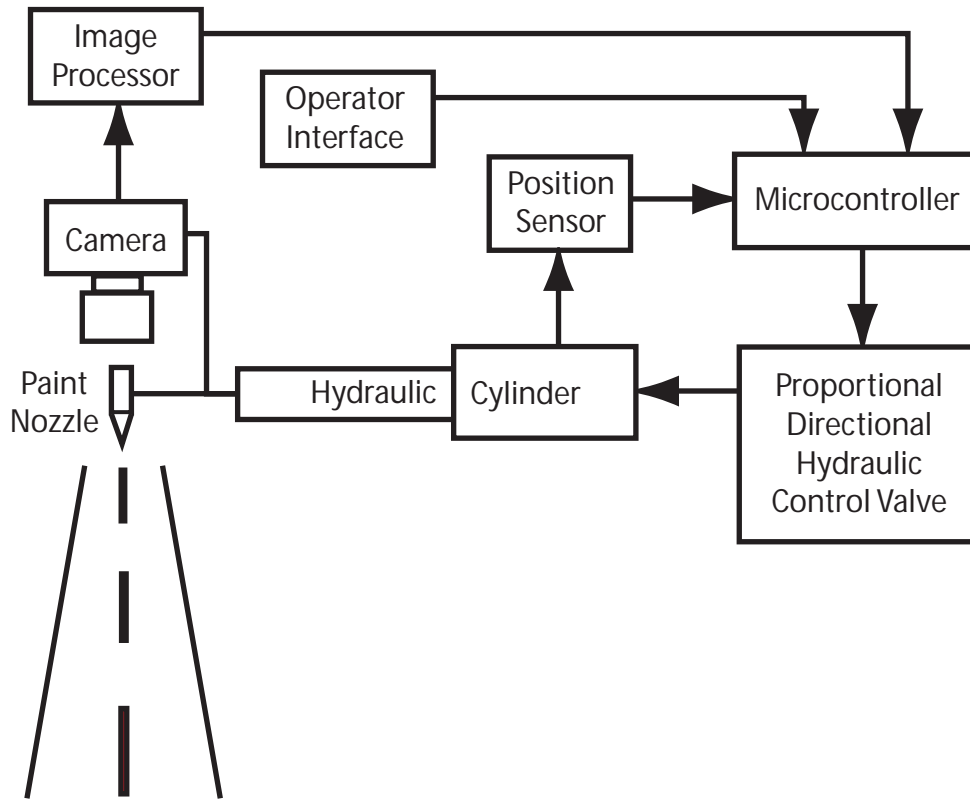


Figure 3. Diagram of lateral position control system for the lane restriping outrigger.

A machine vision system (model Zicam, jointly developed by General Vision, Petaluma, CA and Pulnix America Inc., Sunnyvale, CA) was mounted on the front of the lane restriping outrigger as shown in figures 4 and 5. The options for mounting the machine vision system were constrained by the limited free space on the striping vehicle (especially on the port side of the vehicle) and that no significant mechanical modifications were to be made to the striping vehicle. The machine vision system was mounted inside a 30.5 cm x 25.4 cm x 12.7 cm (12 in x 10 in x 5 in) protective enclosure that was attached to a space on the forward side of the outrigger. A preliminary evaluation was conducted to investigate both a top view (looking straight down) of the roadway and a forward perspective view (similar to the driver's view) of the roadway. A 6 mm wide angle lens (model 60607, F1.2 Cosmocar/Pentax) was selected as the best compromise between maximizing the field of view and minimizing distortion, given the limited options for camera mounting locations. The top view had a field of view of 53.3 cm x 48.3 cm (21 in x 19 in) while the perspective view covered a region 7.6 m (25 ft.) in front of the outrigger.



Figure 4. Machine vision system mounted inside the white enclosure attached to the edgeline outrigger on the starboard side of the striping vehicle with the outrigger in the normal operating position.

The scene in figure 7 is typical of restriping operations on two lane roadways where shadows are common due to trees (or roadway signs) along the edge of the road. In addition shadows caused by the vehicle itself may result in non-uniform illumination of the lane markings. Non-uniform lighting like that shown in figure 7, presents a challenge to machine vision systems because the limited dynamic range of current video camera technology degrades white stripe recognition in scenes where the stripe is partially shaded. The top view was selected in preference to the perspective view because in addition to shadows (which affect both views) the perspective view could be subjected to poor viewing conditions and false stripe detection associated with glare from the pavement when the vehicle was driven toward the sun with the sun at a low elevation and with a larger field of view it was not realistic to mechanically shade this section of roadway.

Figure 6 shows the interior of the machine vision enclosure (the white box shown in figures 4 and 5) and displays the dual Zicam<sup>2</sup> systems in their final configuration. Although only one can

---

<sup>2</sup> Additional information regarding the Zicam system can be found in Appendix B of this report.

be seen in this figure (because the rear camera head is hidden behind the front camera head), there are two camera heads, one mounted directly behind the other in the lower right-hand side of the enclosure. The glass window at the bottom of the enclosure was about 28 inches (71 cm) above the roadway. Each camera head was connected to one of two ZISC (Zero Instruction Set Computer, General Vision, Petaluma, CA) processing units shown on the left side of figure 6. Together a camera head and a ZISC processing unit comprise a Zicam machine vision system. The lens and shutter speed of one of the Zicam systems was adjusted for viewing portions of the roadway in direct sunlight, and the lens and shutter speed of the other was adjusted to optimize the view of the shadowed portions of the roadway. In that way the two systems together could overcome the current limitations of video camera technology to provide a system that was more robust to non-uniform illumination. If in time, improved camera sensor technology becomes available one of the Zicams could be eliminated reducing the cost of the system. One of the Zicam systems was designated as a “master” and the other as a “slave. The two Zicam systems were interconnected and were interfaced to the microcontroller shown in figure 3.

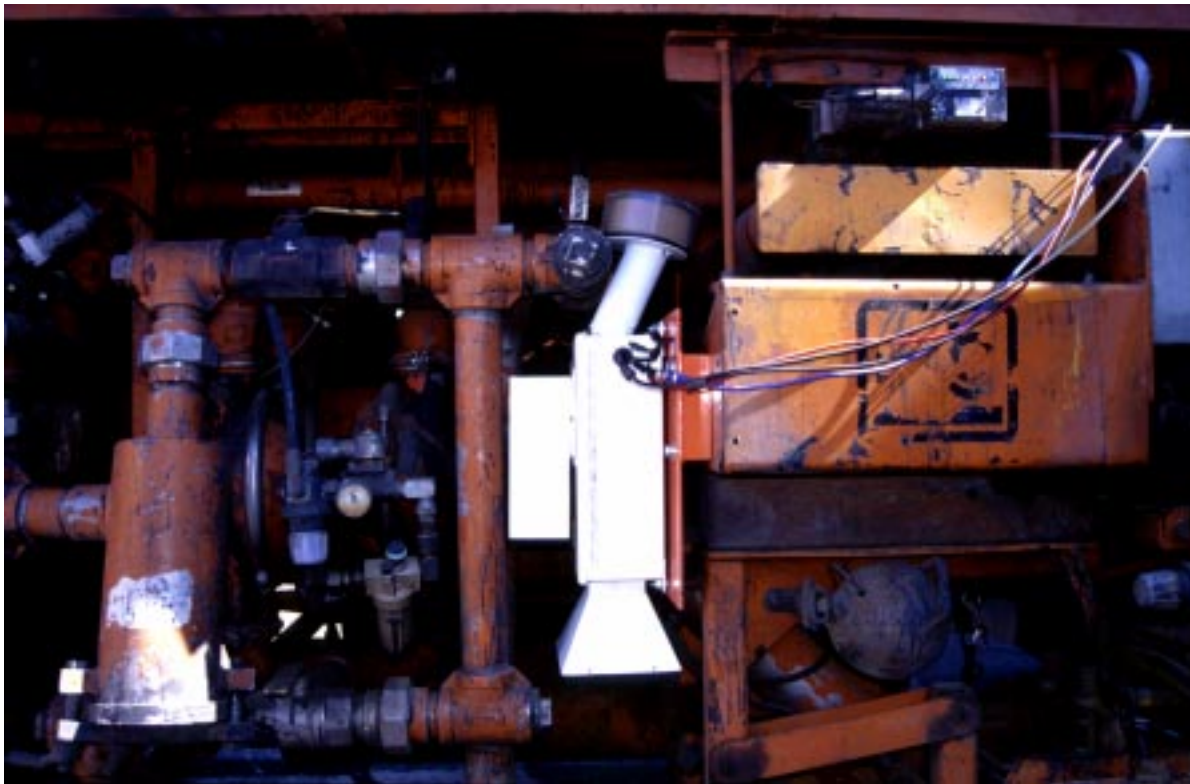


Figure 5. Machine vision system mounted inside the white enclosure attached to the centerline outrigger on the port side of the striping vehicle with the outrigger in the retracted (non-operating) position for storage or high-speed transport.



Figure 6. Enclosure interior showing the configuration of the two Zicam machine vision systems.



Figure 7. View from the rear operator's window showing the port outrigger in operation and shadows caused by trees adjacent to the roadway.

The Zicam enclosure was designed to allow forced air ventilation for cooling and to prevent paint spray drift from accumulating on the camera lenses. A filtered air intake is shown at the

top of the enclosure in figures 5 and 6 and was designed to fit within the vehicle space constraints without modification to the striping vehicle. The viewing window at the bottom of the enclosure was designed to provide an “air wash curtain” across the outside of the window to prevent drifting paint particles from attaching to the window. A flared metal shield was attached to the enclosure, further protecting the window from spray paint drift. CAD type drawings of all enclosure and Zicam mounting hardware are found in Appendix A.

## PRINCIPAL OF ZICAM OPERATION FOR LATERAL OUTRIGGER GUIDANCE

A typical top view Zicam image of a worn lane stripe is shown in figure 9a. The Zicam employs a neural network type computer architecture designed to mimic the pattern recognition ability of the human brain. Each Zicam contains two of General Vision’s ZISC036 chips, each of which contains 36 silicon neurons, for a total of 72 neurons. The silicon neurons within a Zicam are all interconnected and each neuron can be “taught” to recognize a portion of a visual pattern. The neurons work collectively to recognize a specific pattern, in this case a method was developed to train the network to recognize worn patches of lane stripe. The ZISC036 chips have 64 possible inputs to the network. The ZISC036 is a three layer neural network (an input layer, a hidden layer and an output layer). The ZISC036 takes 3.2 ms to process 64 inputs and an evaluation can be achieved within 0.5 ms after the last component has been input to the network allowing 250,000 evaluations per second (this is equivalent to 2.2 giga PC type instructions/s).

A two step process is used to successfully train the Zicam to recognize worn lane stripes. The first step is to develop a method of extracting visual features from the image in figure 9a that can be used to identify the worn lane stripes. Once the visual features have been identified, they are used to train the neural network. The Zicam uses a radial basis function type neural network. An example showing how the radial basis function would map (classify) a visual feature space with two features is shown in figure 8. This example shows two categories, A, which might represent a part of the image that contains no stripe and B representing an area that does contain the stripe. Point (P1, P2) shown in figure 8 represents the knowledge of the visual characteristics for category A that was embedded in the network through prior training. Point (V1, V2) is a new point to be classified by the network. If the new point (V1, V2) lies within the influence field of an existing point (point (P1, P2) in this case) it is classified into the category (category A in this case) of that point. New knowledge can be used to fill in the empty gaps in the feature space or to redefine the size of the influence fields of existing points in the feature space.

The visual feature shown in figure 9 is used by the Zicam for lane stripe recognition and is called the “vertical profile”, where “vertical” in this case was defined as the direction perpendicular to the lane stripe and although horizontal in real life is “vertical” when the image is displayed on a

computer screen. The vertical profile is the intensity of each pixel (picture element) in a vertical line through the image. In general, the intensity of light reflected from the unpainted roadway will be lower than that reflected from a lane stripe and this difference in intensity can be used by the neural network as a visual feature to identify the location of the lane stripe in the image. The spectral reflectance curves typical of unpainted asphalt, and fresh (not worn) white and yellow paint used by Caltrans for lane striping are shown in figure 10. Except for the blue region of the spectrum (where the yellow paint has a low reflectance) the reflectance of both types of paint are similar and consistently higher than the unpainted asphalt. Because the reflectance curves of the paint are basically flat above 570 nm, there is no advantage to using a color or multispectral camera in this situation and the Zicams use a monochrome sensor with the typical silicon CCD spectral sensitivity shown in figure 11. By their nature worn lane stripes however, will not have a consistently higher intensity than the surrounding unpainted roadway. To minimize the effect of the variability in reflectance due to worn paint the Zicam determines the vertical profile not from a single column of pixels, but from the average of several columns of pixels in the image.

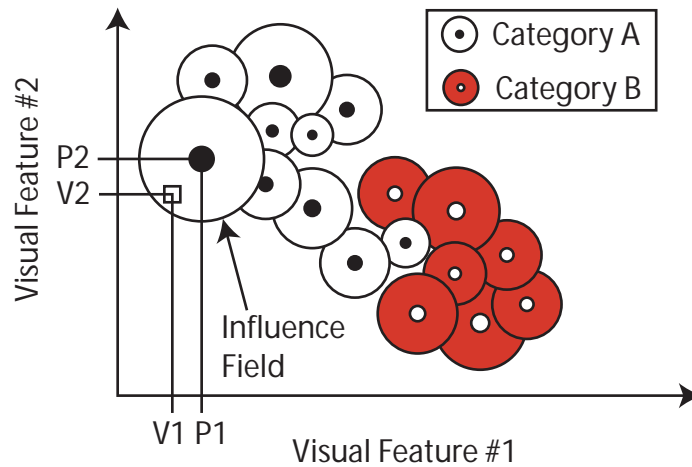


Figure 8. An example of a Radial basis function mapping, where (P1, P2) is stored knowledge from prior training and (V1, V2) is a new visual input to be classified by the network.

The effect of averaging reduces the random error associated with irregular wear patterns or cracks in the pavement and if applied to the entire image it would cause the scene shown in figure 9a to appear like the image in figure 9c. An example vertical profile across the entire image in figure 9c is shown in figure 9d. The high intensity portion of the vertical profile from picture location 130 to 190 in figure 9d is associated with the lane stripe in figure 9c. The visual feature input to the ZISC036 neural network is the average vertical profile from the yellow

rectangular region shown in the box labeled “Image Control” in figure 1 on page 6 of the Zicam manual in Appendix B.

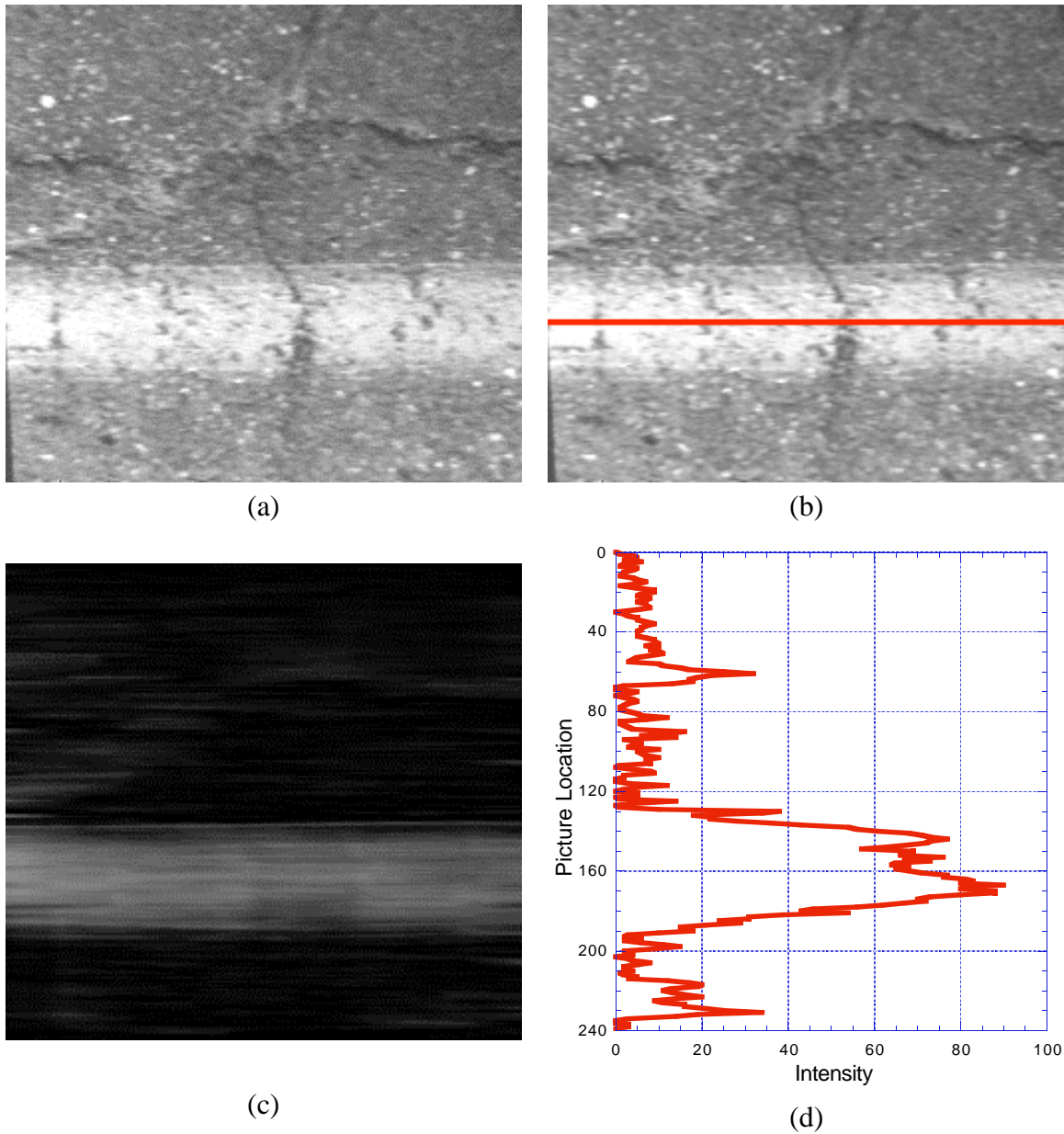


Figure 9. A raw image of a worn edgeline collected from the Zicam is shown in (a), the image in (c) is the result of averaging columns of pixels from (a) to reduce the intensity variation in (a) due to wear and cracks, the graph in (d) is the vertical profile of the intensity in a column from (c), the red line in (b) is the estimated center of the lane stripe using the vertical profile from (d).

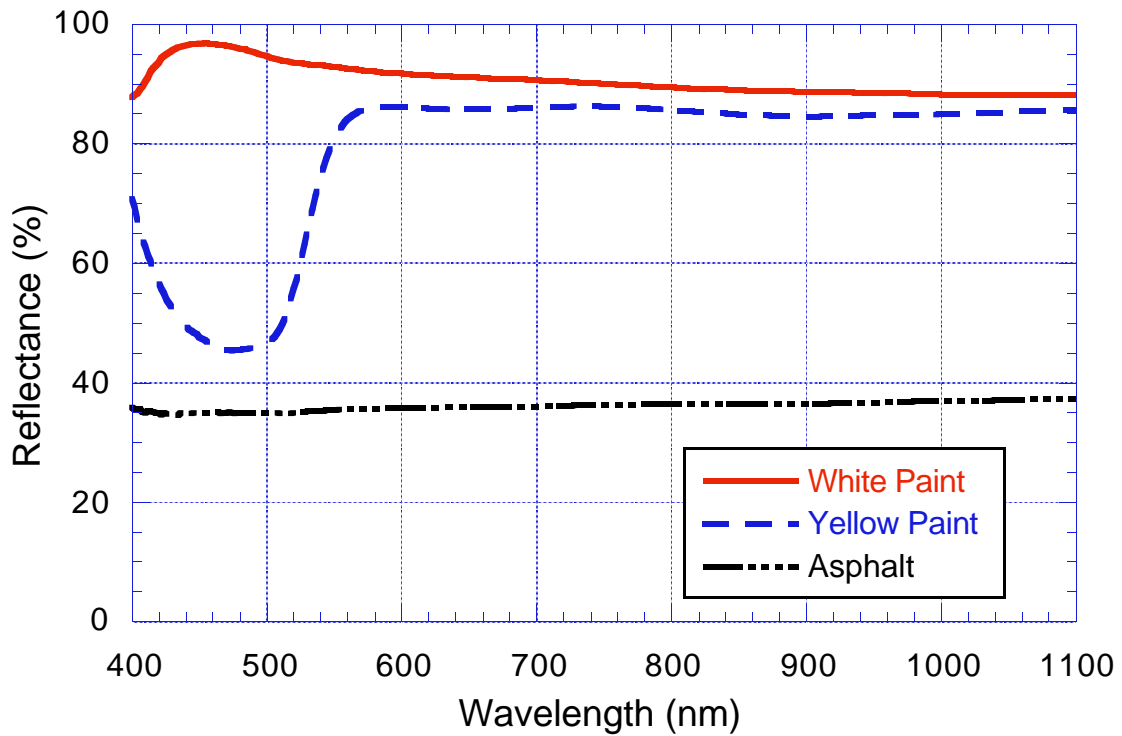


Figure 10. Spectral reflectance curves for fresh white and yellow paint and worn asphalt.

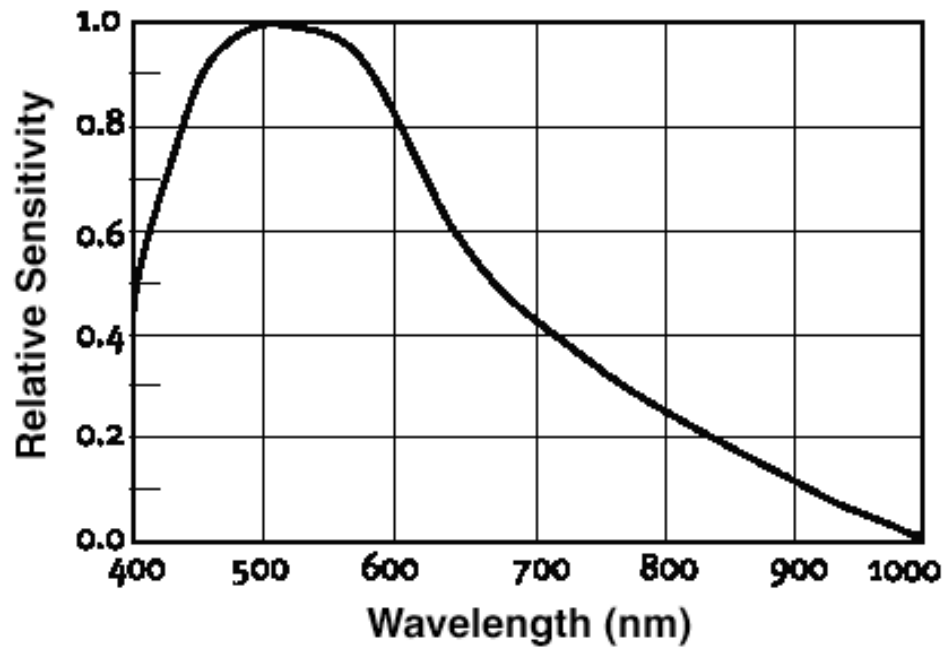


Figure 11. Typical spectral sensitivity of a monochrome CCD video camera.

Once the Zicam has been trained to recognize the difference in the vertical profile from a region of roadway that does not contain the lane stripe versus one that does contain the stripe it can use this information to estimate the location of the center of the lane stripe. The red line shown in figure 9b is the estimated centerline location estimated from the vertical profile.

Once the Zicam has identified the centerline location of the worn stripe to be repainted, it sends this information<sup>3</sup> to the microcontroller shown in figure 3. The new centerline information is used as the new position setpoint in the closed loop lateral position control of the outrigger. The microcontroller position control loop operates at a rate about 100 times greater than the Zicam update rate. In operation, the Zicam continuously repeats the following steps: acquire a new image, extract the vertical profile from a series of potential stripe locations in the image, input these visual features to the ZISC036 neural network, determine the center of the stripe from the vertical profiles identified as belonging to a worn stripe, transfer the stripe centerline information to the microcontroller.

#### SYSTEM RESPONSE REQUIREMENTS FOR LATERAL OUTRIGGER GUIDANCE

To determine the minimum machine vision response rate required for outrigger guidance a video recording was made of the outrigger position accuracy when the striping vehicle was operated by an inexperienced driver without the aid of the normal guidance mirror (seen in figure 1) attached to the striping vehicle. The striping vehicle was operated along a section of winding roadway and the relative position of the outrigger with respect to the lane stripe was determined manually using the program interface shown in figure 12. These conditions were selected to determine the maximum response rate demanded from an automated machine vision guidance system.

A plot of the worst-case lateral outrigger position error is shown in figure 13. In general, the maximum outrigger error was about +/- 60 mm (+/- 2.4 inches) over a period of about 12 seconds under these conditions. For reference, Caltrans' tolerance in lateral restriping error is +/-13 mm (+/- 0.5 inches). A spectral analysis of the outrigger lateral position was conducted and the resulting power spectral density is shown in figure 14. These results show that the lateral motion of the striper falls below a frequency of 0.4 Hz with most of the motion below 0.2 Hz. To achieve an acceptable level of performance in controlling the lateral position of the outrigger, the machine vision system should operate at a minimum rate about 10 times greater than the lateral oscillation of the striper or at a rate above 4 Hz in this case.

---

<sup>3</sup> The communication protocol used by the Zicam to communicate with the microcontroller is described on page 10 of Appendix B. The symbol MB is used in Appendix B for the microcontroller.

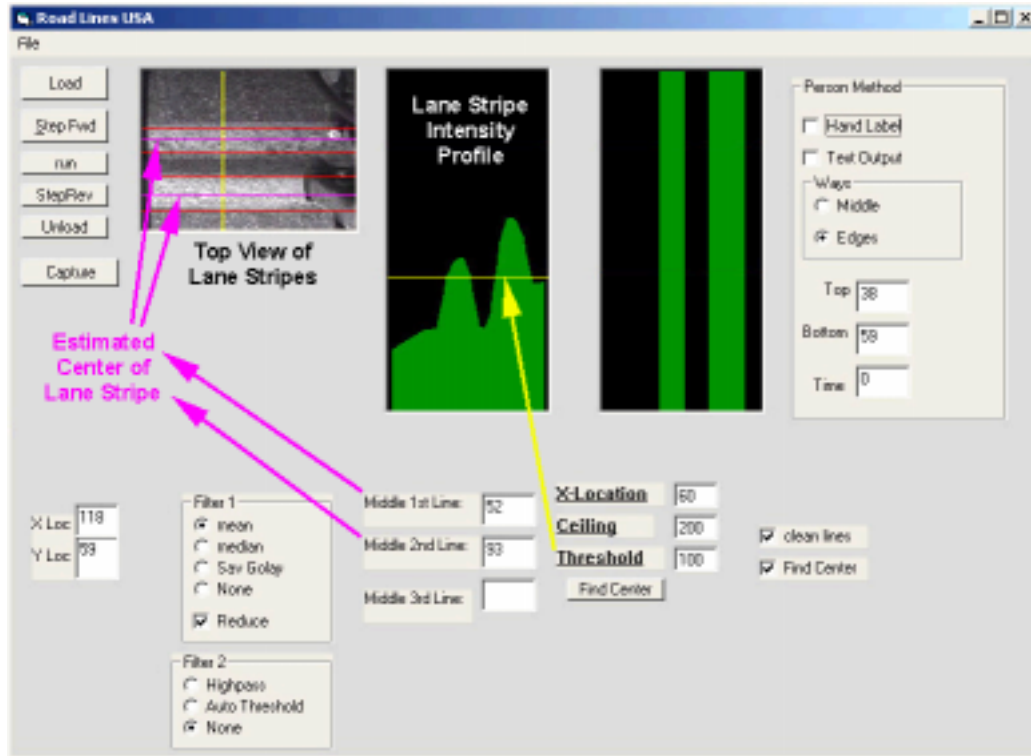


Figure 12. Visual Basic program interface used to determine the relative position error of the outrigger when operated without the automatic guidance system.

The performance of an automatic guidance system is a function of both the sensor and the dynamic response of the actuator, which is the outrigger's hydraulic cylinder in this case. A step test was conducted to evaluate the dynamic performance of the outrigger and to determine the optimum gain settings for automatic feedback control. A PID (proportional, integral, and derivative) control algorithm was programmed into the microcontroller shown in figure 3. The step test was conducted on both the starboard and port outriggers with the step demand moving each outrigger from a position 11.9 inches (30.2 cm) away from the storage position to a position 19 inches (48.3 cm) away from the storage position and then repeating the step test in the opposite direction. The step test result for the starboard outrigger using the optimum gain settings is shown in figure 15. For both outriggers it was determined that neither integral nor derivative control provided superior control to proportional control alone. Figure 16 shows a comparison plot of the step test results for several proportional gains and a test with both proportional and derivative gain, where  $k_p$ =proportional gain,  $k_d$ =derivative gain,  $k_s$ =integral gain, and  $v_z$ =valve zero setting. A 12-bit digital to analog (D/A) converter is used by the microcontroller to output the control signal to the hydraulic control valve. In theory the valve spool should be centered (stopping the motion of the outrigger) with a D/A value of 2048 (half

the maximum 12-bit value), however there was some internal leakage flow through the valve and some spool offset was required to stop the motion of the outrigger. For example, we determined that a D/A value of 2083 was required to offset the internal leakage across the spool and stop the motion of the starboard outrigger.

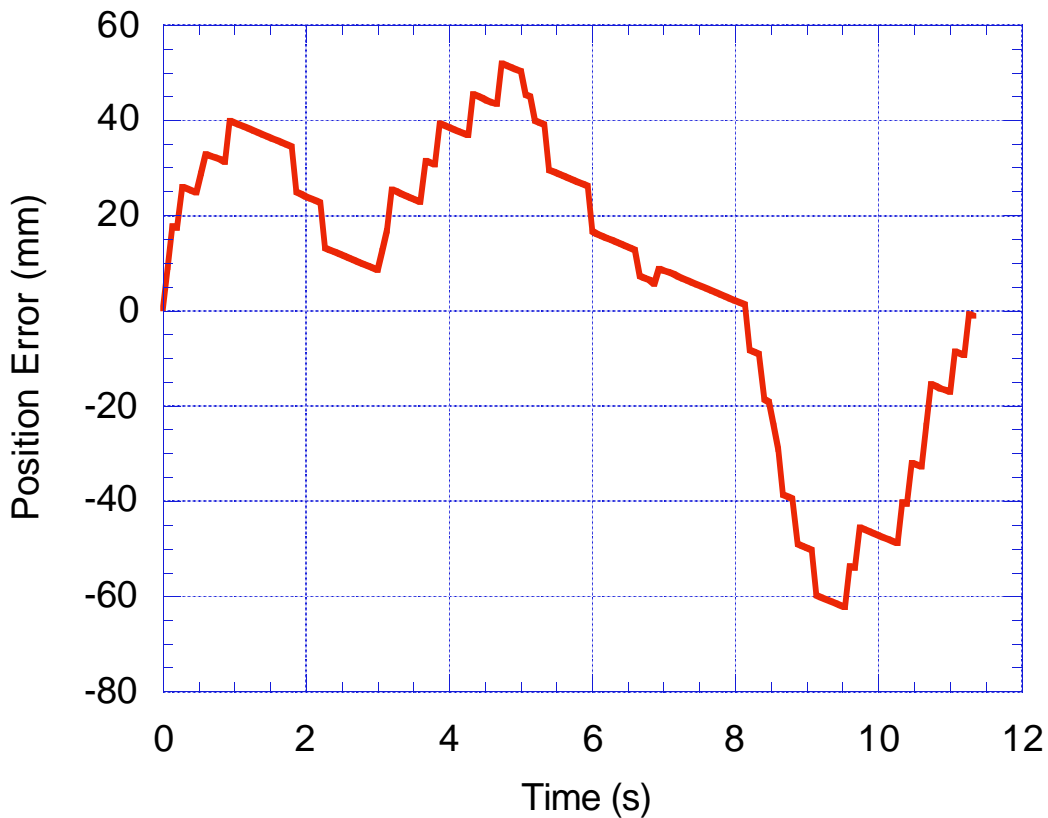


Figure 13. Lateral position error of the outrigger when the striping vehicle was operated by an inexperienced driver without the aid of the guidance mirror seen in figure 1. An error of zero indicates that the paint nozzle is located directly above the center of the lane stripe.

In general, it was observed that under optimum conditions the outrigger performance under proportional closed-loop feedback control could travel at a speed of about 7 inches/second (18 cm/s). The maximum demand observed in figure 15, when the striping vehicle was operated by an inexperienced driver without the aid of the guidance mirror seen in figure 1, was about 2.4 inches/second (6 cm/s). This level of demand is about one third the maximum speed of the outrigger indicating that the dynamic performance of the outrigger under proportional

closed-loop feedback control should be capable of providing satisfactory performance once a satisfactory lateral guidance sensor is available.

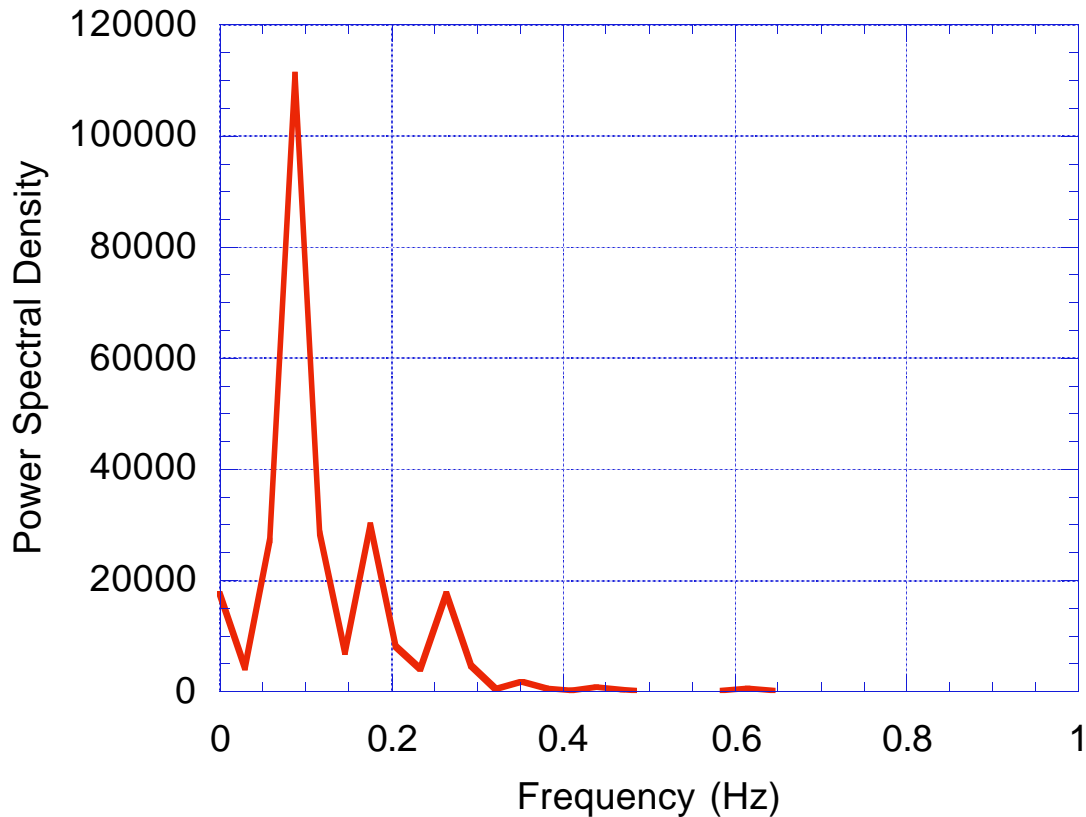


Figure 14. Power spectral density of the outrigger position when the striping vehicle was operated by an inexperienced driver without the aid of the guidance mirror.

#### ZICAM DEVELOPMENT CHRONOLOGY AND PERFORMANCE EVALUATION

After significant manufacturing delays the first functional Zicam system was installed on the District 10 striping vehicle in September 2000, nine months behind schedule. The system was tested using a simulated worn lane stripe at the UC Davis campus. A movie of the UC Davis test can be found on the CD-ROM disk in the folder in Appendix E. As delivered, the Zicam system did not utilize its field programmable gate array (FPGA) in the feature extraction process and as a result was forced to significantly limit the portion of the image analyzed. General Vision concluded that without utilizing the FPGA the Zicam performance was too slow. In May 2001, General Vision informed UC Davis and Caltrans that their manufacturing cooperator, Pulnix

America Inc., had discontinued further development of the Zicam and that the FPGA programming had not been completed. In June 2001, General Vision abandoned the development of the Zicam and decided to develop a new machine vision guidance system using a compact computer manufactured by Leutron. Unfortunately, General Vision was unsuccessful in delivering a functional machine vision system, based either on the Zicam design or the Leutron computer before the project ended in September 2001.

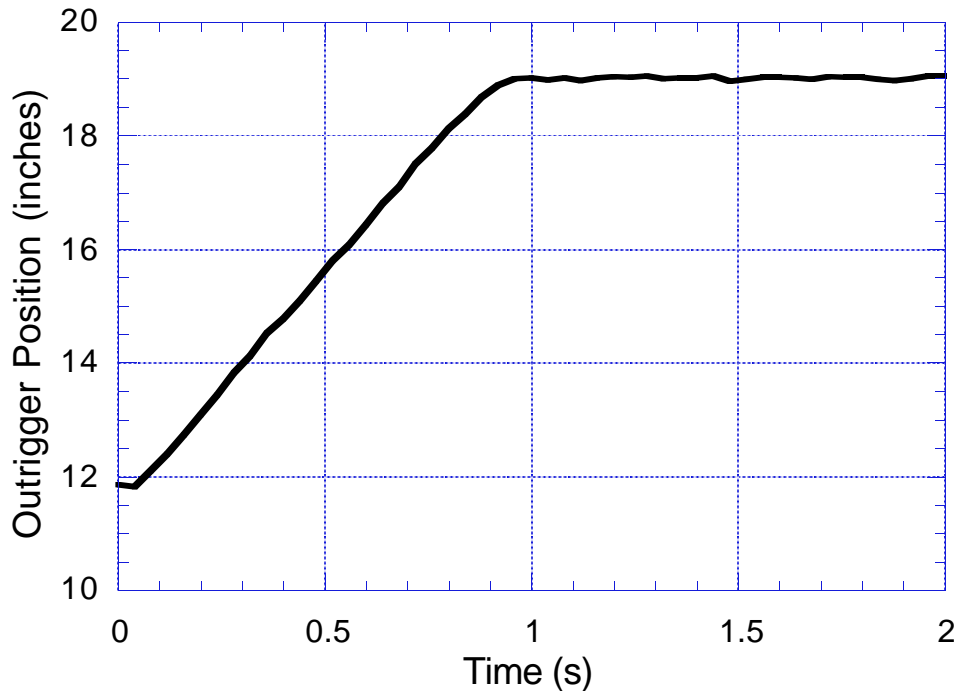


Figure 15. Step test response of starboard outrigger, valve offset = 2083, proportional gain =8.

From the authors' perspective the basic visual extraction technique and use of the radial basis function type neural network to locate the worn lane stripe showed great promise, however the development of the Zicam system was plagued with manufacturing delays. When the project began, the ZISC technology owned by General Vision was considered state-of-the-art, however with time no technological improvements were made and by 2001 gains in personal computer technology had virtually eliminated any technological advantage the ZISC technology previously enjoyed over traditional computing hardware.

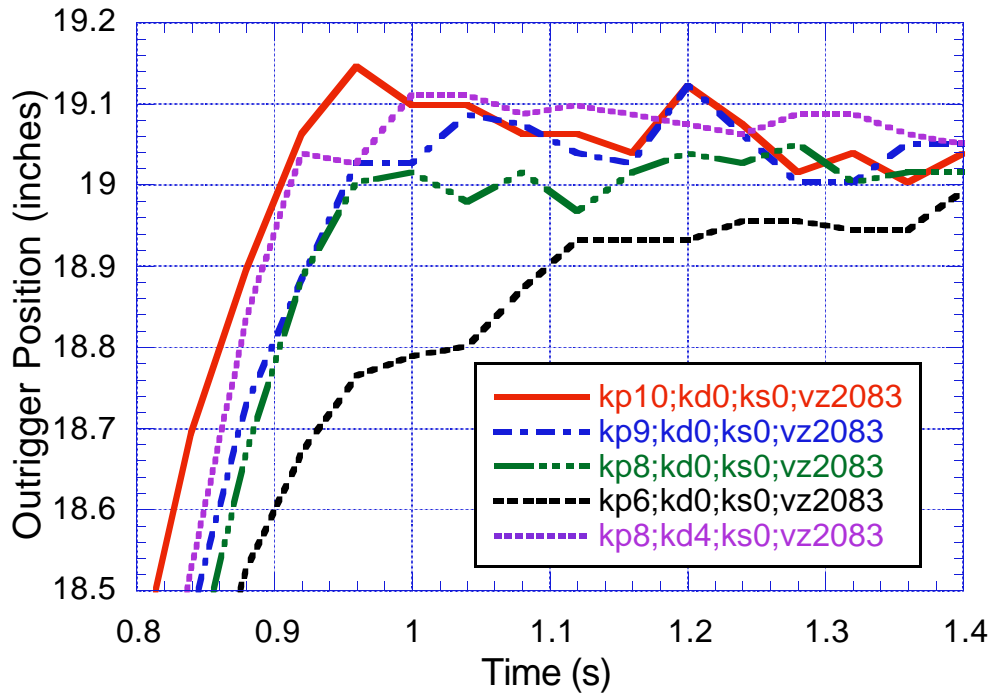


Figure 16. Step test of starboard outrigger showing the effect of changes in proportional and derivative gain levels.

In the summer of 2001, when General Vision abandoned the development of the Zicam and decided to start over with a completely new hardware platform, Caltrans authorized UC Davis to begin a parallel effort to develop, in the limited time remaining, a machine vision guidance system using off-the-shelf machine vision hardware. UC Davis purchased a low-cost, compact, industrial machine vision computer (model 4SightII, Matrox Electronic Systems Ltd., Quebec, Canada) and developed the software needed to recognize worn lane stripes for this system, figure 17. The recognition capabilities of this machine vision system were successfully demonstrated at the AHMCT demonstration held at UC Davis on September 21, 2001. This system was significantly faster than the Zicam and had a price about half the projected selling price of the Zicam. Unfortunately the proportional directional hydraulic control valve on the striping failed (due to age) at this time and the manufacturer no longer manufactured this model. A non-proportional hydraulic valve was used to replace the existing valve. A proportional directional hydraulic control valve is required for automatic guidance and until the correct replacement valve is installed on the striping vehicle field testing was not possible. Due to time limitations and the mechanical failure of the existing proportional directional hydraulic control valve on the striping vehicle this new system could not be tested on the striping vehicle before

the end of the project. Further effort is required to install new proportional directional hydraulic control valves on the lane striping vehicle and begin field testing.

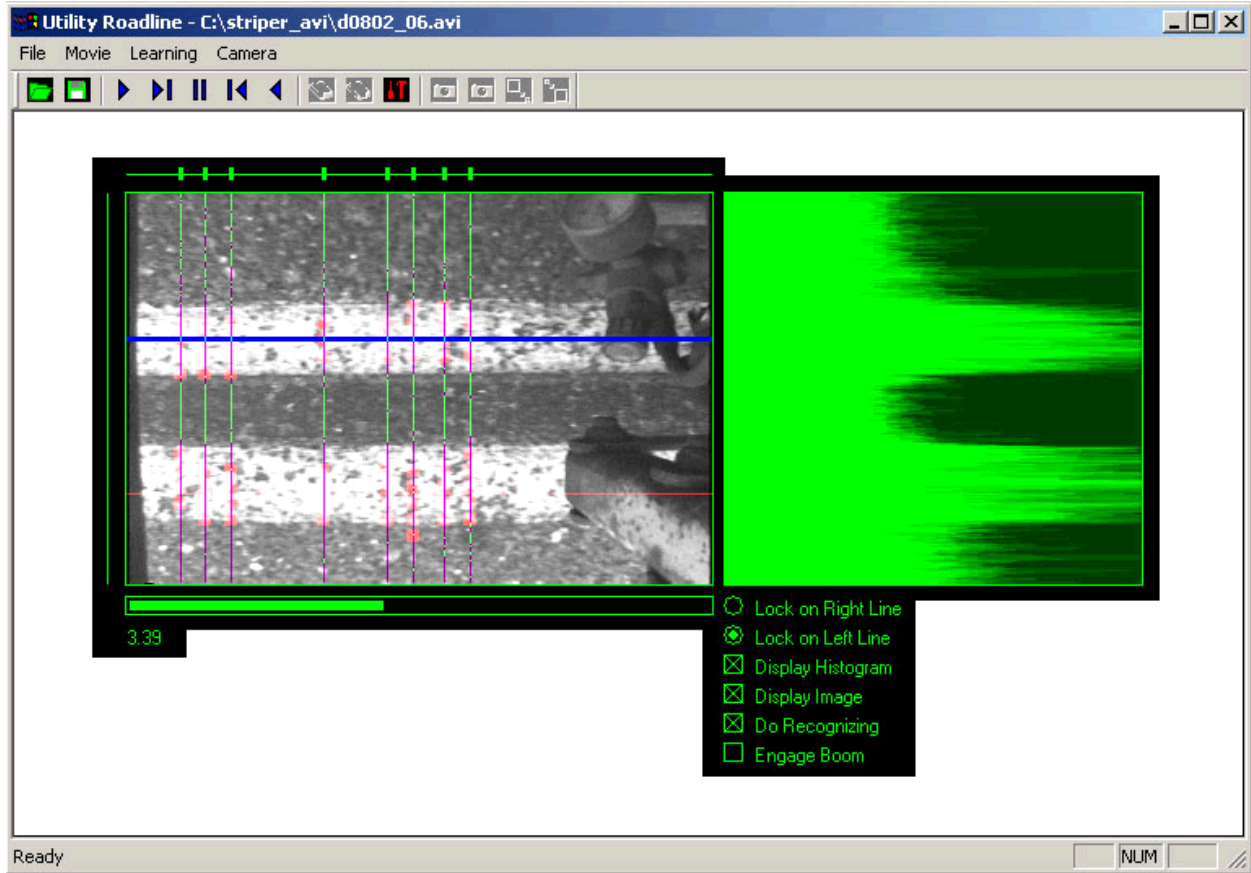


Figure 17. Software interface for automatic recognition of worn lane stripes developed by UC Davis for a standard industrial machine vision computer without the use of the ZISC hardware.

### DASH LENGTH CONTROL SYSTEM

A radar speed sensor (model DRS1000, GMH Engineering, Orem, UT) was mounted beneath the rear deck of the striping vehicle near the existing ground wheel displacement sensor in a manner similar to that shown in figure 1 of the GHM Engineering Application Note 1001 in Appendix C, except that the sensor was mounted facing forward. The sensor emits a 0-5 volt square wave at a rate of 473.3 pulses/m (211.6 Hz/MPH). The sensor output was input to one of the counters on the microcontroller shown in figure 3 of this report. The microcontroller was then programmed to control the paint solenoid based upon the longitudinal (in the direction of travel) displacement

of the striping vehicle as an alternative to the ground wheel displacement sensor normally used to control dash line length. The advantage of the radar sensor is that it is non-contact, and virtually maintenance free. The sensor tested had a weather resistant enclosure, a speed range of 1 to 300 MPH (1.6 to 480 kph) and a temperature range of  $-17^{\circ}\text{C}$  to  $60^{\circ}\text{C}$  ( $0^{\circ}\text{F}$  to  $140^{\circ}\text{F}$ ). It was selected because it was one of the only radar sensors that claimed to be accurate enough to control the dash length within the  $\pm 4$  inch ( $\pm 102$  mm) tolerance Caltrans requires. The manufacture specified that the total unadjusted worst case error of this sensor was  $\pm(0.36\% + 0.0016\%/MPH)$ .

The longitudinal control of the dash length and the length of space between dashes in a dashed paint line were evaluated using the following three methods:

1. Existing encoded ground wheel displacement sensor using the existing longitudinal paint valve controller.
2. Existing encoded ground wheel displacement sensor using the microcontroller shown in figure 3 to control paint valve actuation.
3. Radar displacement sensor using the microcontroller shown in figure 3 to control paint valve actuation.



Figure 18. Striping vehicle conducting a test of the longitudinal accuracy of dash line length.

Each of the three methods of longitudinal control was evaluated using the following two stripe patterns:

1. 2.5-foot (0.76 m) dash with 12.5-foot (3.8 m) space between dashes.
2. 7-foot (2.1 m) dash with 17-foot (5.2 m) space between dashed.

Striping tests were conducted at Caltrans's normal operating speed on the UC Davis campus, figure 18. Each test was 1,200 feet (366 m) in length. After striping, the length of each dash and the length of the space between each dash were recorded manually using a tape measure.

The overall standard error of longitudinal accuracy is shown in Table 1. When the existing encoded ground wheel and the existing controller were used, the dash and space lengths had a 2.6% probability of failing the required  $\pm 4$  inch ( $\pm 102$  mm) length tolerance. When either the existing ground wheel or the radar sensor was used with the microcontroller the dash and space lengths were within  $\pm 3.1$  inches ( $\pm 78.5$  mm) 99.9% of the time and never exceeded the  $\pm 4$  inch ( $\pm 102$  mm) tolerance.

This study did not examine the effect of variations in pavement temperature or air temperature on the accuracy of these two systems. It is expected that the effective diameter of the wheel will change with temperature causing an error in the length of the dashed lines. The effect of temperature on the radar sensor is unknown (although the manufacturer specifies the operating range to be  $-17^{\circ}\text{C}$  to  $60^{\circ}\text{C}$  ( $0^{\circ}\text{F}$  to  $140^{\circ}\text{F}$ )). The study also did not study any long-term effects such as the change in air pressure or rolling resistance in the tire over time that could result in a loss of accuracy.

The advantage of the radar sensor is that it is a non-contact device and has no moving parts. It is expected (but not evaluated in this study) that the radar sensor would have lower maintenance costs than the existing ground wheel. It is also expected (but not evaluated in this study) that Caltrans could reduce the striping variability in longitudinal control of the dash length and the length of space between dashes in a dashed paint line by switching from ground wheel based displacement sensing to radar based displacement sensing because it is expected that a radar sensor would have better long-term calibration stability.

This study showed that the existing dash-length control system is a source of error, which can cause the dashed line length to exceed the tolerance set by Caltrans. The error in dashed line length due to the control system could be significantly reduced by replacing the existing dash-length control system with a modern microcontroller-based system like the one used in this study.

Table 1. Precision of longitudinal control of dash and space lengths.

Existing Wheel & Controller Standard Error (mm)	Existing Wheel & New microcontroller Standard Error (mm)	Radar Sensor & New microcontroller Standard Error (mm)
45.7	25.4	25.4

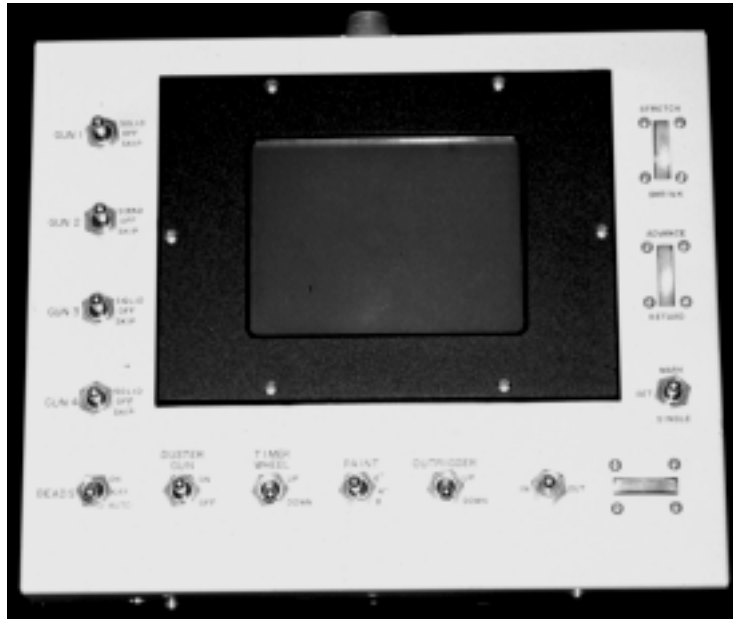


Figure 19. Redesigned operator interface, showing traditional paint valve switches and a new touch screen display.

### OPERATOR INTERFACE

A new operator interface was designed to replace the existing interface for the operator in the rear of the striping vehicle, figure 19. The interface was designed to be more compact making the work space more user friendly and incorporated a touch screen display to allow the operator better access to striping settings. The new interface occupied only 30% of the space required for the existing interface and having a programmable display it is capable of displaying much of the information currently displayed on the center console (near the operators right hand in figure 2). Although the interface software was never finalized due to General Vision's failure to complete the machine vision system, this type of interface has the potential to improve safety, reduce worker stress, and improve restriping efficiency by placing all the controls and operating

parameters in a compact single unit within easy reach of the operator, as opposed to the inefficient and scattered interface shown in the existing system, figure 2.

## CONCLUSIONS AND RECOMMENDATIONS

This report describes a developmental feasibility study for the automatic guidance of a lane restriping system to automatically apply paint on top of worn traffic lane boundary striping with a lateral tolerance of +/-13mm and a longitudinal tolerance of +/-102mm for dashed lane striping. This system would assist the California Department of Transportation in their effort to enhance safety, reduce worker stress, improve restriping efficiency, and reduce traffic flow impacts of striping maintenance. Machine vision recognition systems employing both hardware and software based neural network lane stripe recognition were evaluated. Preliminary results show potential for automatic machine vision location of worn traffic lane boundary striping, however additional field testing is needed to fully evaluate the accuracy of this type of system. The computational power of computer technology continues to increase significantly with time. As this trend continues the ability to automate complex tasks such as outrigger guidance and lane stripe pattern switching using machine vision becomes increasingly feasible. It is recommended that Caltrans continue to study the use of machine vision as a means to enhance safety, reduce worker stress, improve restriping efficiency, and reduce traffic flow impacts of striping maintenance.

A non-contact radar displacement sensor was evaluated for longitudinal control of dash length as an alternative to a traditional ground-driven encoded wheel sensor. The radar sensor was found to operated within the desired longitudinal tolerance and had a standard error of 25.4 mm (1 inch). The advantage of the radar sensor is that it is non-contact, and virtually maintenance free. Further study is needed to evaluate the long-term accuracy of the radar sensor over time and any possible affect of temperature on the sensor. By installing more precise and accurate displacement sensors on all the striping vehicles within each district, Caltrans can reduce the differences in dash length that currently occur between strippers within the same district.

In short tests (i.e., 1,200 feet) it was observed that the existing dash-length control system is a source of error, which can cause the dashed line length to exceed the tolerance set by Caltrans. Further study is needed to determine the level of error caused by the existing dash-length control system over longer time periods and under different environmental conditions such as changing temperature. It is recommended that Caltrans consider updating these older control systems with modern microcontroller-based systems like the one used in this study. By updating the control system the standard error was reduced from 45.7 mm to 25.4 mm in the tests reported in this study.

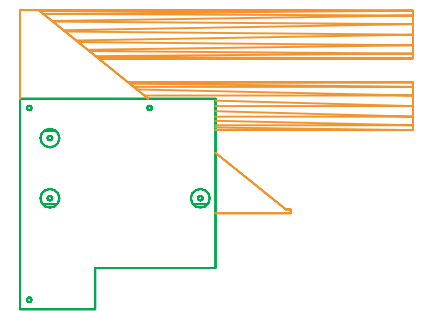
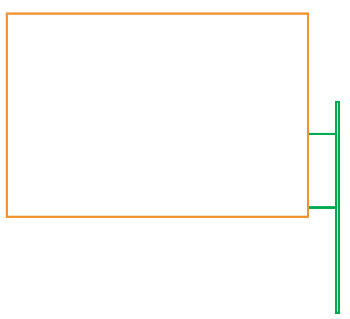
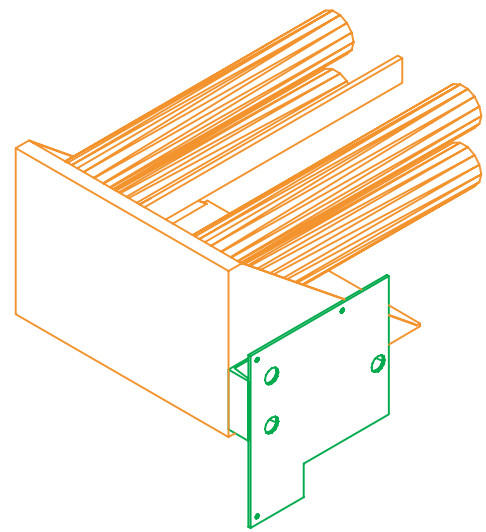
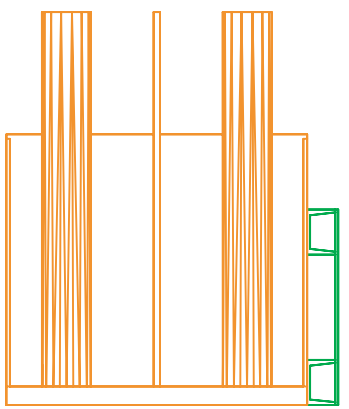
APPENDIX A

CAD DRAWINGS FOR ZICAM ENCLOSURE



REVISIONS

ZONE	REV	DESCRIPTION	DATE	APPROVED
------	-----	-------------	------	----------



Note: Do Not Scale Drawing

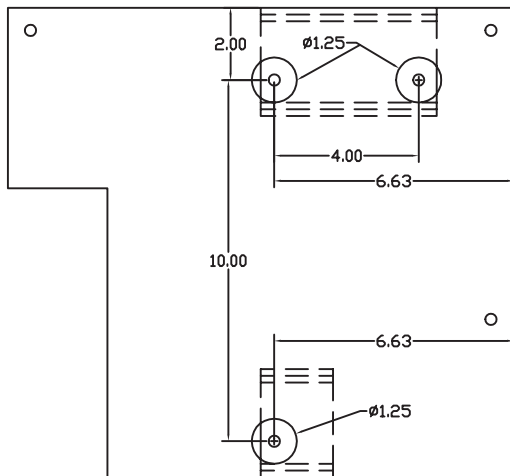
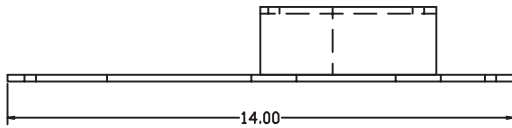
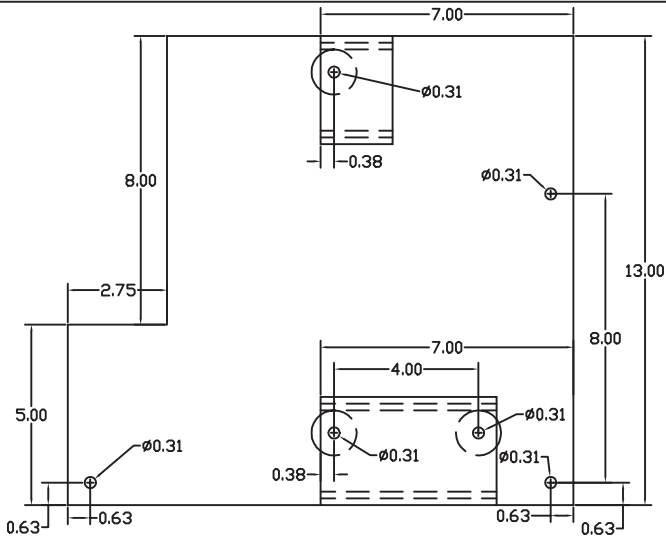
Outrigger  
Camera  
Mounting  
Bracket

Lane Restriping Guidance System Project

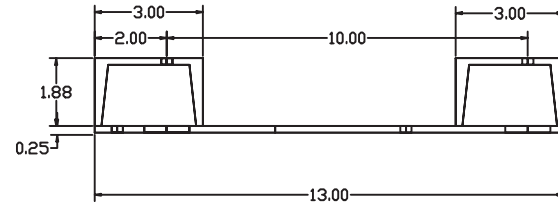
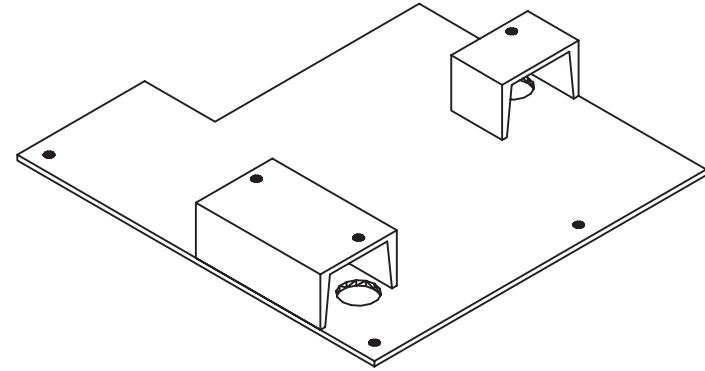
AHMCT / UCDAVIS

SIZE A	FSCM NO.	DWG NO.	REV
SCALE	SHEET		





REVISIONS				
ZONE	REV	DESCRIPTION	DATE	APPROVED



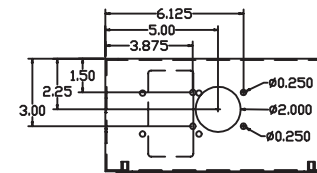
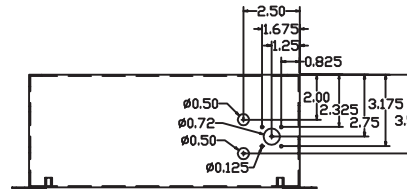
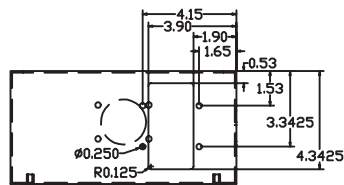
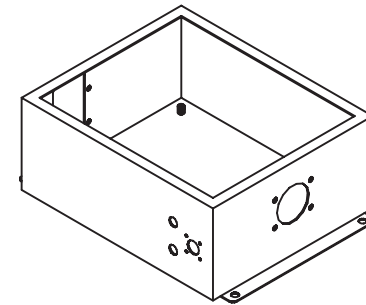
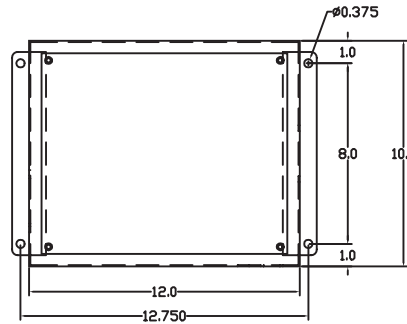
Note: Do Not Scale Drawing

Outrigger Mounting Bracket for Camera	Lane Restriping Guidance System Project			
	AHMCT / UCDAVIS			
Material: Aluminium	SIZE A	FSCM NO.	DWG NO. OutriggerBracket.dwg	REV
	SCALE			SHEET

ZiCAM camera box manufactured from a steel J, type 12, electrical box, model A-1210CH (Hoffman Enclosures, Inc.)

Note: Box lid omitted for clarity, lid hinge on front view.

REVISIONS				
ZONE	REV	DESCRIPTION	DATE	APPROVED



Note: box exterior painted white.

Camera Box Modifications

Lane Restriping Guidance System Project

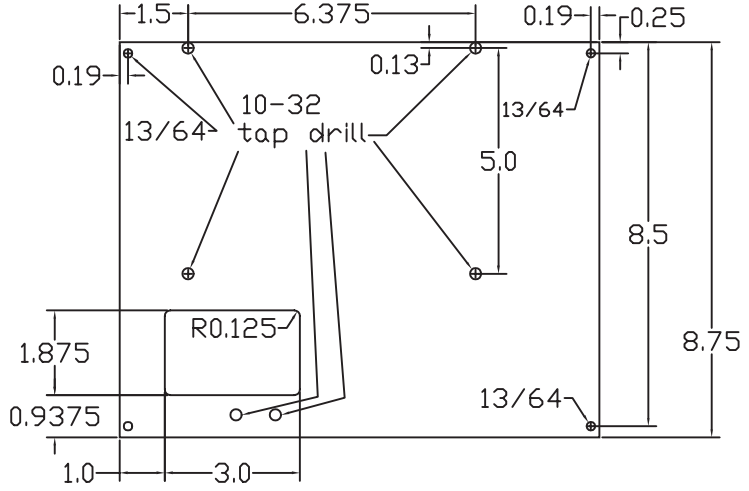
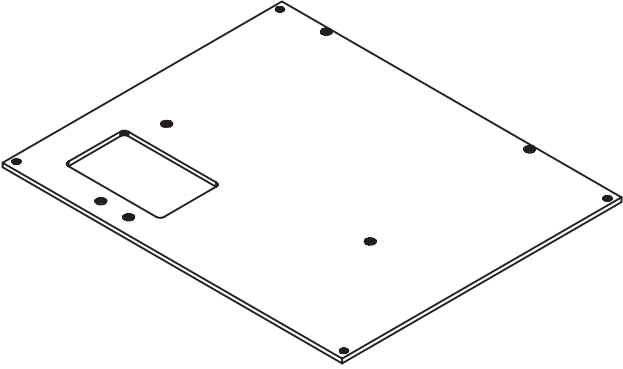
AHMCT / UCDAVIS

SIZE A	FSCM NO.	DWG NO. CameraBoxMods.dwg	REV
SCALE	SHEET		



REVISIONS

ZONE	REV	DESCRIPTION	DATE	APPROVED
------	-----	-------------	------	----------



Camera Box  
Base Plate

Lane Restriping Guidance System Project

Note: Do Not Scale Drawing

AHMCT / UCDAVIS

Material: Aluminium

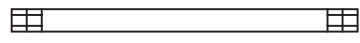
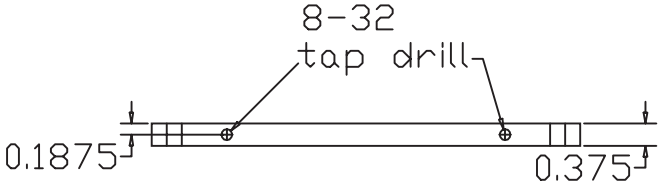
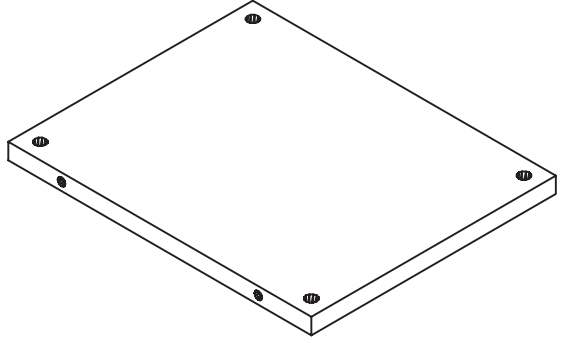
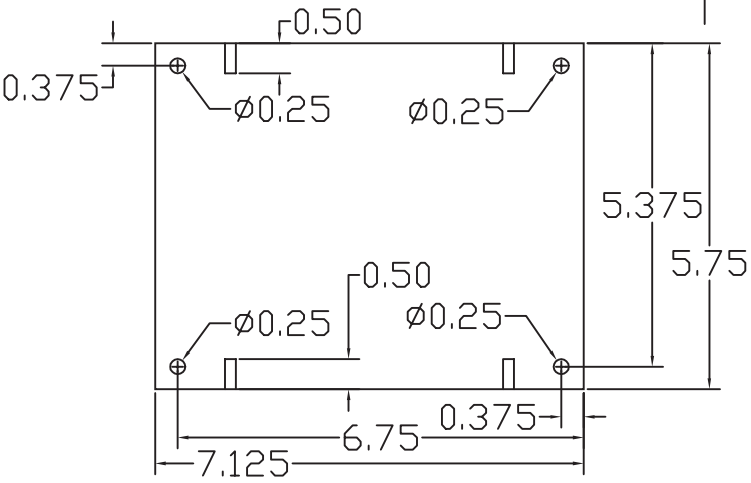
SIZE A	FSCM NO.	DWG NO. BasePlate.dwg	REV
SCALE	SHEET		





REVISIONS

ZONE	REV	DESCRIPTION	DATE	APPROVED
------	-----	-------------	------	----------

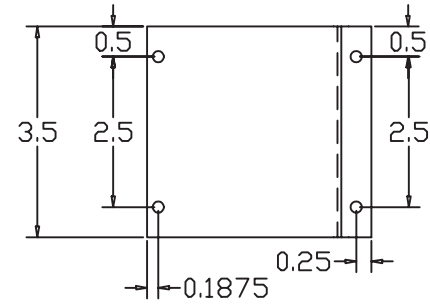
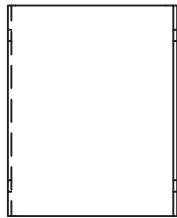
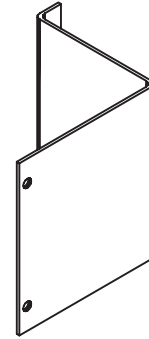
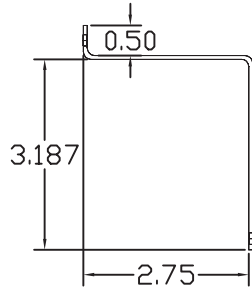


Note: Do Not Scale Drawing.

ZiCAM CPU Mounting Plate		Lane Restripping Guidance System Project		
		AHMCT / UCDAVIS		
Material: Aluminium	SIZE A	FSCM NO.	DWG NO. ZiCam_Plate.dwg	REV
	SCALE		SHEET	



REVISIONS				
ZONE	REV	DESCRIPTION	DATE	APPROVED



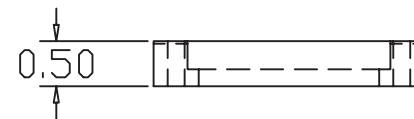
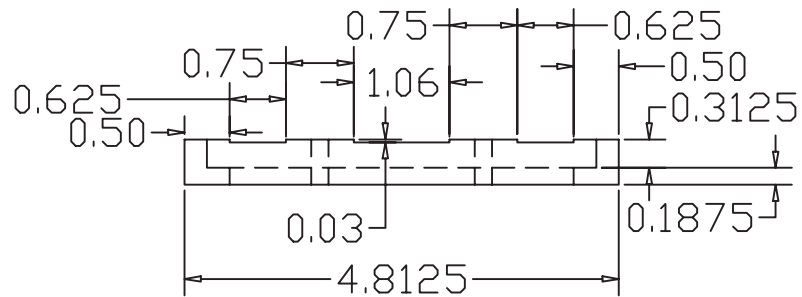
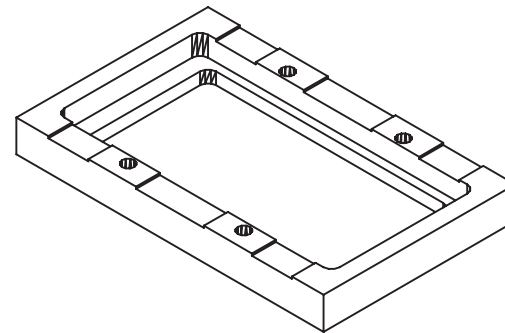
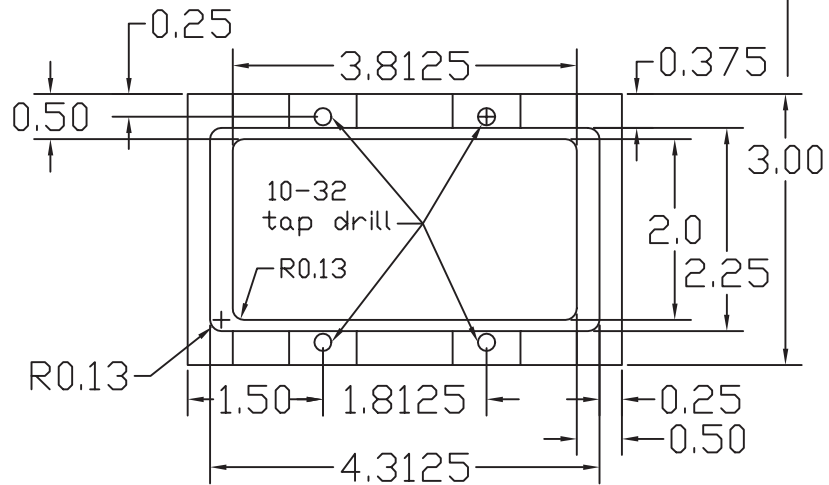
Note: Do Not Scale Drawing  
20 gage sheet metal.

ZiCAM CPU Clamps		Lane Restriping Guidance System Project		
		AHMCT / UCDAVIS		
Material: sheet metal	SIZE A	FSCM NO.	DWG NO. ZiCam_Clamp.dwg	REV
Quantity: 2	SCALE	SHEET		



REVISIONS

ZONE	REV	DESCRIPTION	DATE	APPROVED
------	-----	-------------	------	----------



Note: requires 1/16 by 1/4 by 2 rubber strip between window and box at each end.

Note: Do Not Scale Drawing

Window glass retainer

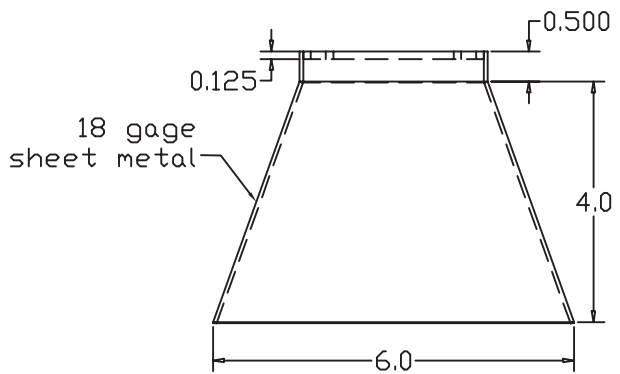
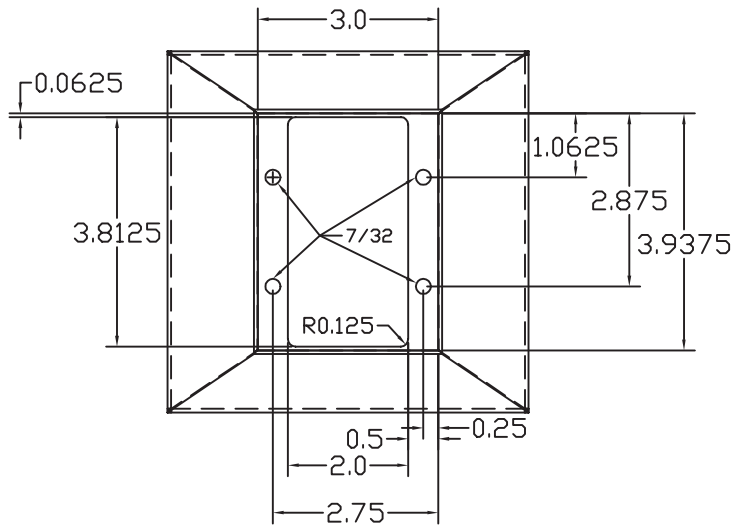
Lane Restriping Guidance System Project

AHMCT / UCDAVIS

Material: Aluminium

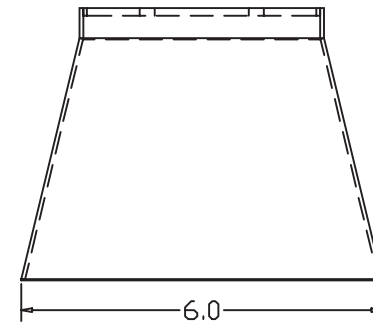
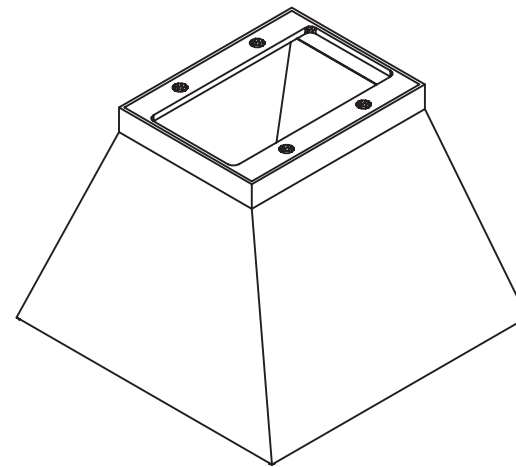
SIZE A	FSCM NO.	DWG NO. WindowRetainer.dwg	REV
SCALE	SHEET		





Note: Do Not Scale Drawing  
Paint outside white  
and inside black.

REVISIONS				
ZONE	REV	DESCRIPTION	DATE	APPROVED

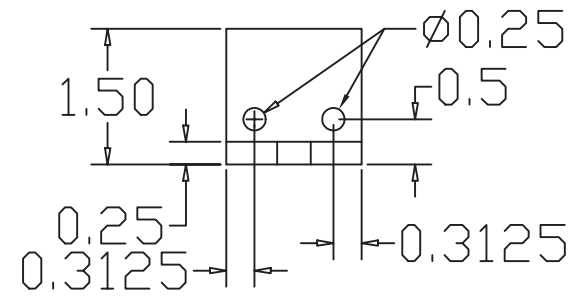
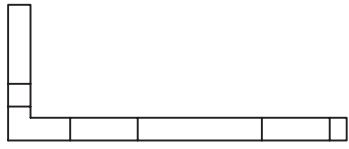
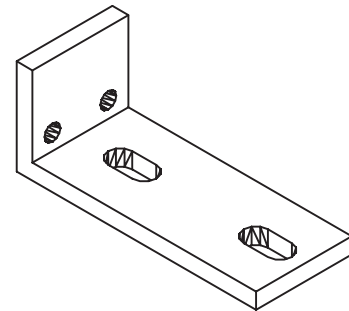
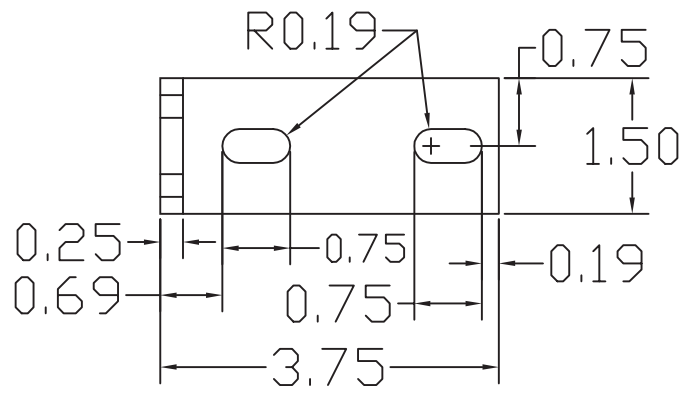


Camera Window Paint Shield	Lane Restriping Guidance System Project			
	AHMCT / UCDAVIS			
Material: Steel	SIZE A	FSCM NO.	DWG NO. PaintShield.dwg	REV
	SCALE		SHEET	



REVISIONS

ZONE	REV	DESCRIPTION	DATE	APPROVED
------	-----	-------------	------	----------



Note: Do Not Scale Drawing

Camera Head Mounting Bracket	Lane Restriping Guidance System Project			
	AHMCT / UCDAVIS			
Material: Aluminium	SIZE A	FSCM NO.	DWG NO. CameraBracket.dwg	REV
	SCALE			SHEET



APPENDIX B

ZICAM MANUAL

# **Zicam Guidance System (ZGS)**

Manual

Version 1.2  
Revised 1/01 by General Vision Inc.

Chapter A . Hardware Description.....	3
1 ) What's in the Zicam ? .....	3
2 ) Zicam Back Panel .....	4
Chapter B . Software .....	5
1 ) Zicam Instructor (PC interface) .....	5
2 ) Zicam Resident Software (Firmware).....	8
Chapter C . Communication Protocol .....	10
1 ) Interface specifications.....	10

## Chapter A . Hardware Description

The ZGS system consists of two remote head Zicam smart cameras from PULNiX. A picture of the ZGS system mounted on the outrigger of the Caltrans lane restriping truck can be seen in figure 2.

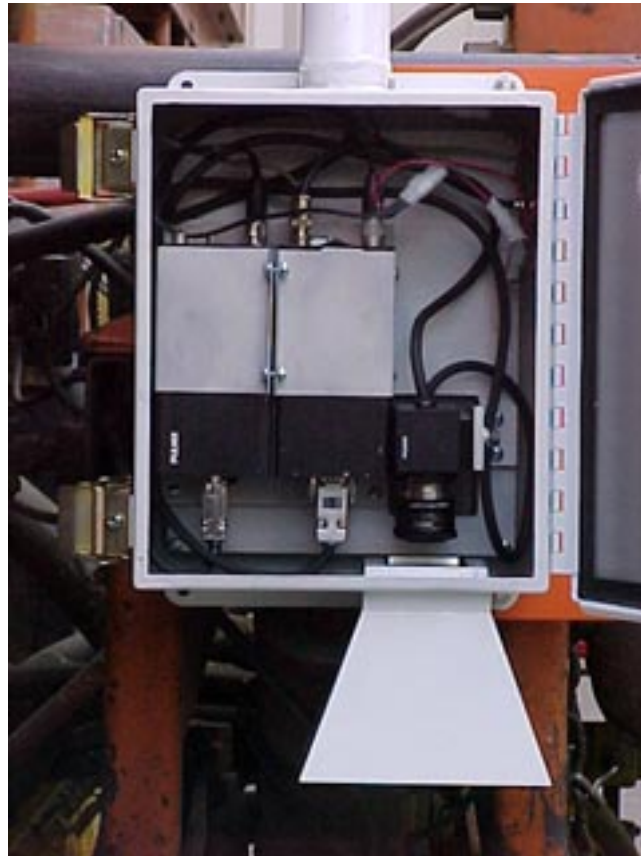


Figure 2. The ZGS system mounted on the Cal Trans Truck.

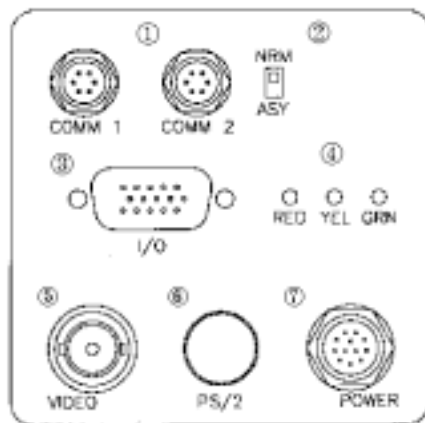
### 1) What's in the Zicam ?

The Zicam has three computer boards. The first board is a CCD camera board for the 648 x 484 pixel progressive scan CCD sensor. The second PCB board is a Multimedia Recognition Engine (MUREN). The Muren board has a Field Programable Gate Array (FPGA), two banks of 1 megabyte each of DRAM, and 2 Zero Instruction Set Computing (ZISC36) chips. The third computer board in the Zicam is the CPU board. The CPU board

has a Motorola 68340 CPU and is responsible for command and control of the Zicam operation as well as all serial and digital communications through the back panel. The CPU board also has two PCMCIA slots. A 340 Mega-Byte MicroDrive from IBM is installed in one of the PCMCIA slots. The MicroDrive can be used to save images and restore them for later use if desired.

The Zicam hardware is built by PULNiX of America. Detailed information about the hardware inside of the Zicam can be obtained from PULNiX.

## 2) Zicam Back Panel



### 1. 6-Pin RS-232C Connector

Pin#	Description	Pin#	Description
1	RxD	4	N/C
2	TxD	5	N/C
3	N/C	6	GND

### 2. Mode Switch

NRM/ASY switch  
(Manual shutter and Asynchronous shutter switch)

### 3. 15-Pin I/O

Pin#	Description	Pin#	Description
1	In1 (Anode)	9	Out2
2	In2 (Anode)	10	Out3
3	In3 (Anode)	11	Out4
4	In4 (Anode)	12	Out5
5	In5 (Anode)	13	Out6
6	N/C	14	Out7 (Option)
7	GND	15	Out8 (Option)
8	Out1		

Pin#0, 9 and 10 can be configured by jumper pins as either PNP or NPN open collector output. As default, all output pins are configured as NPN type.

### 4. LED Indicator

RED: Power Indicator  
YEL: Inspection Fail  
GRN: Inspection Success

### 5. Analog Video Out

### 6. PS/2 Keyboard

Pin#	Description	Pin#	Description
1	KBD Clock	4	N/C
2	GND	5	+5V DC
3	KBD Data	6	N/C

### 7. 12-Pin Power Connector

Pin#	Description	Pin#	Description
1	GND	7	N/C
2	+12VDC	8	N/C
3	N/C		
4	N/C		
5	N/C		
6	VINIT In		

Figure 3 Zicam Back Panel

## Chapter B . Software

This Section describes the Zicam Guidance System (ZGS) software. Two sets of custom software are utilized in the operation of the ZGS. The first piece of software (firmware) resides in the ZGS and is the actual operating software for the ZGS. The second piece of software (Zicam Instructor) resides on a PC and interfaces with the ZGS through a RS232 serial link. Zicam Instructor is the software tool that is used to “train” the ZGS. Once the ZGS is trained, the Zicam Instructor RS232 link is disconnected and the ZGS runs independent from the PC.

### 1) Zicam Instructor (PC interface)

The Zicam Instructor should be installed on a desktop or laptop PC connected by RS232 serial link to the Zicams Comm1 Port. Minimum specifications for the host PC of Zicam Instructor should be Pentium 233 MHz or higher with 32 MB ram running windows 98 or higher. The Zicam instructor is used to set various ZISC parameters and teach the ZGS different line types. In order to teach the ZISC a line, the BNC output of the Zicam should be connected to a multisync monitor. Upon power up, the live image from the Zicam sensor should be displayed on the multisync monitor. Appropriate multisync monitors (model # 38-V42IIA-A2) are available from PULNiX Inc. (408) 747-0300.

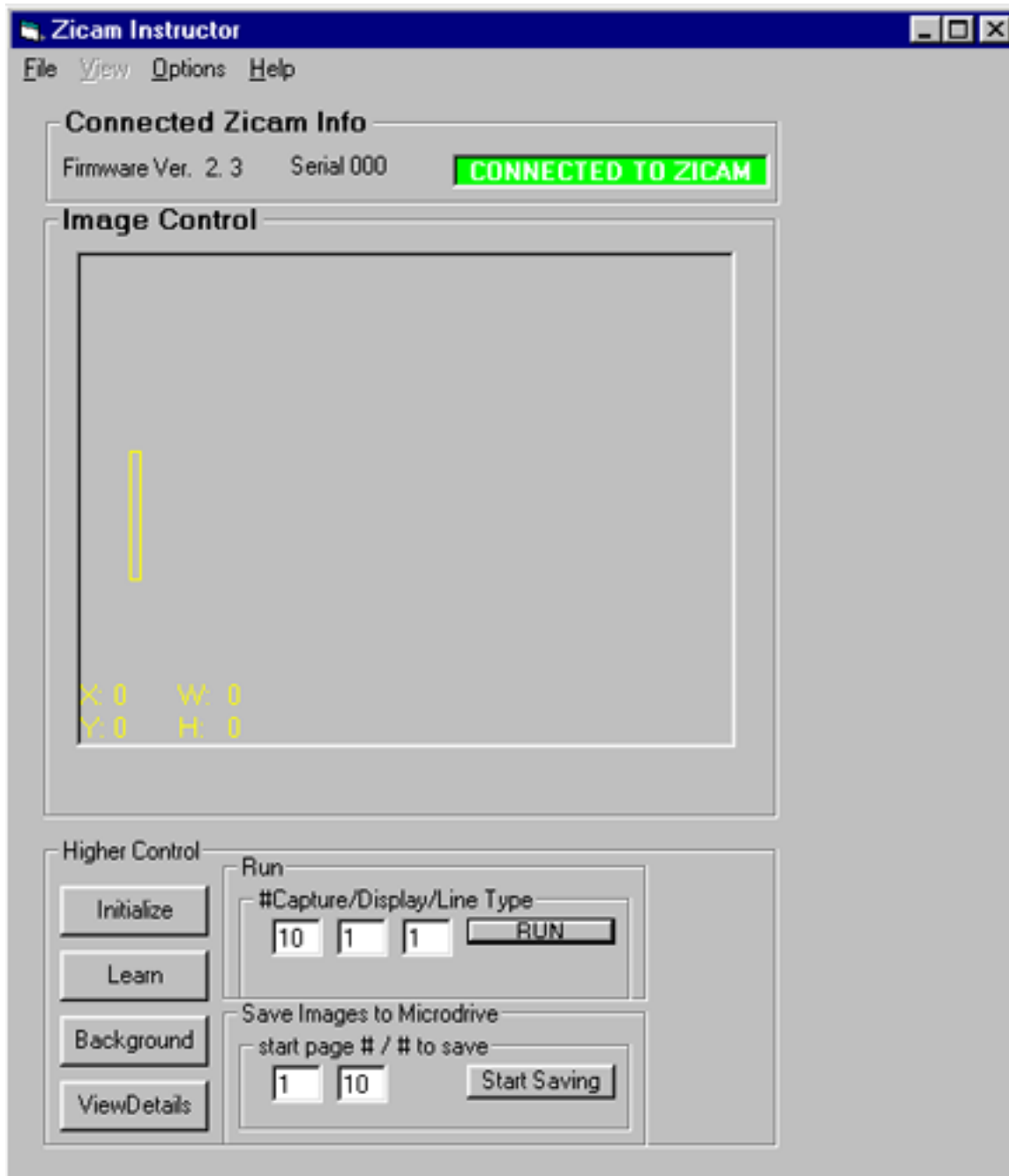


Figure 1 Zicam Instructor user interface.

Once Zicam Instructor is started it tries to establish serial communication with the Zicam. If communication is established, the words “CONNECTED TO ZICAM” will appear in green in the Connected to Zicam Info box. If connection is not established, the words “Zicam not connected” will appear.

Once communication is established, the Zicam Instructor needs to Initialize the Zicam. You can do this by clicking on the Initialize button in the higher control box of the Zicam Instructor. During initialization, the Zicam Instructor will grab a picture from the Zicam and display it in the Image Control picture box.

Now the Zicam instructor is ready to teach the Zicam to recognize a road line. You can place the Region of interest (ROI) (the yellow rectangle in the picture box) over the line to be learned. You can move the ROI by placing the mouse over the left side of the rectangle, left click and drag. You can resize the ROI by selecting the right side or bottom of the ROI, left click and drag.

Once you have placed the ROI over the line, you can click on the “Learn” button. The Zicam takes a sample of the image from the ROI location and performs a feature extraction on the pixels in this region. The firmware is set to use the “Vertical profile” feature extraction technique for line recognition. After learning the sample, the system will display the learned pattern and the total number of neurons committed on the multisync monitor connected to the Zicam BNC output.

Now you can click on the “Run” button in the RUN box of the Zicam Instructor and have the system run for the predetermined number of iterations in the box labeled “# Capture” at the far left of the RUN Button. The default number of iterations is 10. While the system is running, you can see the positively found line regions on the output of the multisync monitor.

If the system is either too liberal or too conservative in its recognition of road lines, the parameter SMINMAX can be used to adjust the systems level of “liberalness”. You can click on the button “View Details” on Zisc Instructor to view the parameter SMINMAX. The default value of SMINMAX is 1200. This is the ZISC Maximum influence field. If you would like to make the system more liberal, just increase this number and re- Initialize the system. If you want the system to be more conservative, reduce the Max influence field and re- Initialize the system (re-training is required after re-initialization).

After the learning phase, you can save the knowledge on the Zicam's micro drive by selecting "Save Zicam Parameters" under the File menu of the Zicam Instructor. If you choose to save the parameters to Bank 1, this knowledge base will be loaded automatically upon power up of the Zicam.

## 2) Zicam Resident Software (Firmware)

The ZGS firmware is developed in ANSI C and compiled by the Diab TM Data compiler software for the Motorola 68340 CPU. Upon compilation an SRE file is created. The SRE file is the compiled file that may be uploaded to the Zicam through a RS232 serial link on COMM1 of the Zicam. A program is available from PULNiX called Z\_uploader that can automatically upload the new SRE file.

Table 1 Operation of the ZGS system.

Step	Outrigger Control Computer	ZGS Master Camera	ZGS Slave Camera
1)	Send 'S' and 'RUN'	Receive 'S' and 'RUN' in comm1	Receive 'S' and 'RUN' in comm1
2)		Send 'Z2Start' out comm2	Receive 'Z2Start' in comm2
3)	Send MB control byte	Receive MB control byte	
4)			Capture Image
5)		Capture Image	Scan through image looking for line "hits" and generating a hit list. (Scan Algorithm)
6)		Scan through image looking for line "hits" and generating a hit list. (Scan Algorithm)	Calculate Line center
7)		Calculate line center	
8)		Receive Slave camera line center information in comm2	Transfer line center location out comm2
9)		Calculate Master line center location	
10) Goto step 4	Receive line center location	Send master line center location out comm1	

\*MB refers to the control computer in the CalTrans truck.

The scan algorithm listed in step 7 of the ZGS Master Camera and step 6 of the ZGS slave camera is the method by which the ZGS determines where the line resides in the images. The default parameters with which the system scans through the images are as follows:

Max, min Influence field 1200, 2

Feature Extraction technique = Vertical Profile

Region of interest size (ROI) = 4 by 60 pixels

Step X, Y = 20, 10

Region of Scan (ROS) SX,EX,SY,EY = 10,280,0,180

The Feature Extraction technique is the method by which the system extracts information from the image pixels and assembles them for recognition by the ZISC chip. Vertical Profile is the average value of the columns of pixels in the ROI. The  $i^{\text{th}}$  component of the feature vector is equal to the average value of the pixels in the  $i^{\text{th}}$  row of the ROI. The vertical profile is a relevant feature to characterize patterns oriented horizontally such as stacked materials, layers and horizontal lines.

The ROS is important because it defines where in the image the ZGS will search for the line. The origin of the image 0,0 is with respect to the upper left corner of the image. The start location in the X direction is SX, the start location in the Y direction is given by SY. The end locations in the X and Y directions are given by EX and EY respectively. The default values can be modified by clicking on the view details button in the Zicam Instructor interface prior to initialization.

# Chapter C . Communication Protocol

## 1) Interface specifications

The ZGS system communicates to the outrigger control computer through a RS232 connection. The ZGS has a female DB9 connector. The baud rate is 38400 with 8 data bits, 1 stop bit, no parity and no flow control.

Upon power up, the ZGS requires an ascii "S" and "RUN" in order to initialize and begin searching for lines. The outrigger control computer should supply the "S" and "RUN" upon power up. After power up, standard consistent communication should transfer between the ZGS and the outrigger control computer as follows. The camera should send messages to the outrigger control computer at a rate of 10 to 100 Hz. The outrigger control computer will respond to each message sent by the camera.

	bit 7-----bit 0
Camera to MB...	OS7   OS6   OS5   OS4   OS3   OS2   OS1   OS0
	0   0   0   RDY   L3   L2   L1   L0
MB to Camera...	0   0   CIC   0   L3   L2   L1   L0

OS0-OS7 is the offset. It is sent by the camera as a 2's complement number. RDY is generated by the camera. It is set to 1 when the camera is locked onto the line and therefore ready to assume control of the outrigger. L0-L3 is the line type. This is generated by the MB side. CIC is generated by the MB side. It is set to 1 to indicate that the camera is in control of the outrigger.

Line types:

- 0 - Manual control of outrigger
- 1 - Double solid
- 2 - Single solid
- 3 - Single dashed
- 4 - Left passing (solid right, dashed left)
- 5 - Right passing (solid left, dashed right)

## APPENDIX C

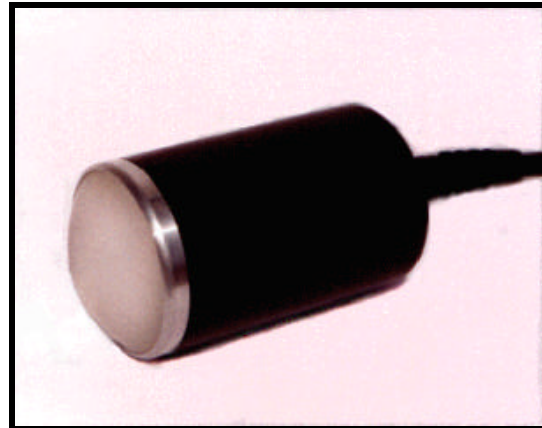
### RADAR SENSOR SPECIFICATIONS

The Delta Speed Sensor is an inexpensive, non-contact Doppler radar speed sensor suitable for a wide variety of applications. Small and lightweight, it requires only a small DC power source, making it ideal for situations requiring portability or remote sensing.

The Delta Speed Sensor may be placed on a moving vehicle or mounted stationary. It can measure surface speeds, such as vehicle ground speed or it can be used to measure the speed of a moving target. The target can be anything from a wire passing under the sensor to a vehicle a thousand feet away.

The output of the sensor is a pulse with frequency proportional to measured speed. The aggregate number of pulses may also be used to determine surface length or distance traveled.

The sensor can be used with GMH Engineering's DataBRICK Data Acquisition System or SRO100 Programmable Digital Indicator. It can also interface directly with many different types of off-the-shelf hardware, such as digital tachometers, or can be integrated into electronic control or data acquisition systems.



## Features

- Non-contact speed measurement
- Inexpensive
- Digital pulse output automatically enabled according to signal strength or target presence
- Small, lightweight
- Low power requirement
- Weather resistant

## Typical Applications

- Vehicle ground speed measurement
- Amusement park ride testing
- Conveyor belt operations
- Motion sensing
- Speed control
- Traffic monitoring
- Length or Distance Measurements

---

### Contact Information: GMH Engineering

336 S. Mountain Way  
Orem, UT 84058  
(801) 225-8970  
www.gmheng.com

FAX: (801) 225-9008  
Email: info@gmheng.com

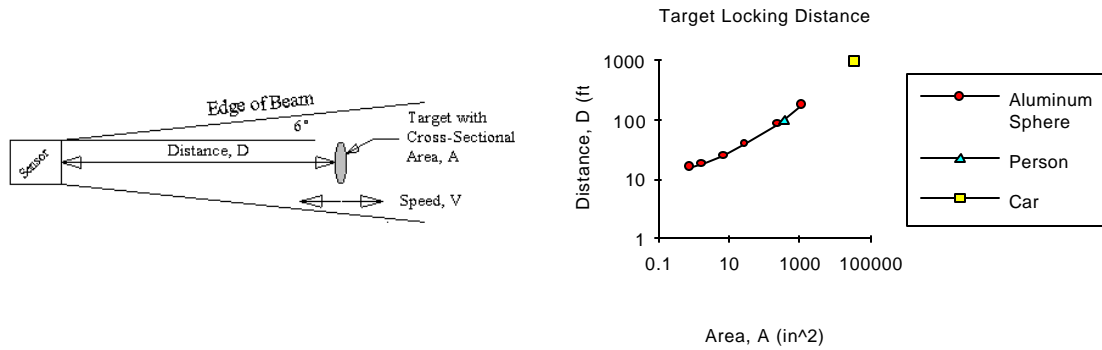


Figure 1 -- Locking Test Diagrams: Target moving along beam center axis (0° velocity offset angle)

## Specifications

Output: 0-5V square wave, differential line driver; 100 Hz/MPH <sup>1</sup>

Max. Target Distance: over 1000 ft. (305 m.)  
(See Figure 1 - Locking Test)

Update Period: 0.01 sec.

Microwave Characteristics: <sup>3</sup>

Frequency: Ka Band 35.5 ± .1 GHz,  
Beam Divergence Angle: 6° from center  
Average RF Power: 0.02 W max  
Effective Radiated Power: 0.98 W

Speed Measurement:

Range: 1-300 MPH  
Total Unadjusted Error: <sup>2</sup>  
± (0.34% + 0.0023%/MPH)

Power Supply: 10.5 - 16.5 VDC, 2.4 W

Sensor Response:

Locking Latency: 0.02 sec.  
Unlocking Latency: 0.05 sec.  
Sensor Time Constant: 0.025 sec.

Temperature Range: 0 to 140°F (-17 to 60°C)

Enclosure: Weather resistant

Weight: 0.5 lb. (230 g)

- Notes: <sup>1</sup> Output requires cosine correction for any offset angle between target direction of travel and beam center axis.  
<sup>2</sup> i.e.: ±0.34% @ 1MPH, ±0.49% @ 65MPH, ±1.03% @ 300MPH (this is for sensor only - overall accuracy of speed measurement is also influenced by external factors such as alignment, vibration, clutter, etc.)  
<sup>3</sup> Regulated under FCC regulations Part 90, Subpart F. Contact GMH Engineering for details.

## Physical Dimensions and Electrical Interface

Wiring: Red: Power +  
Black: Power -  
Green: Signal +  
White: Signal -

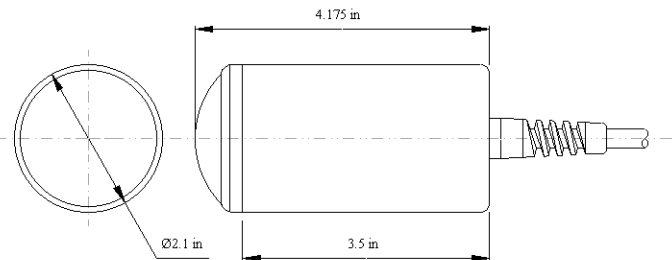
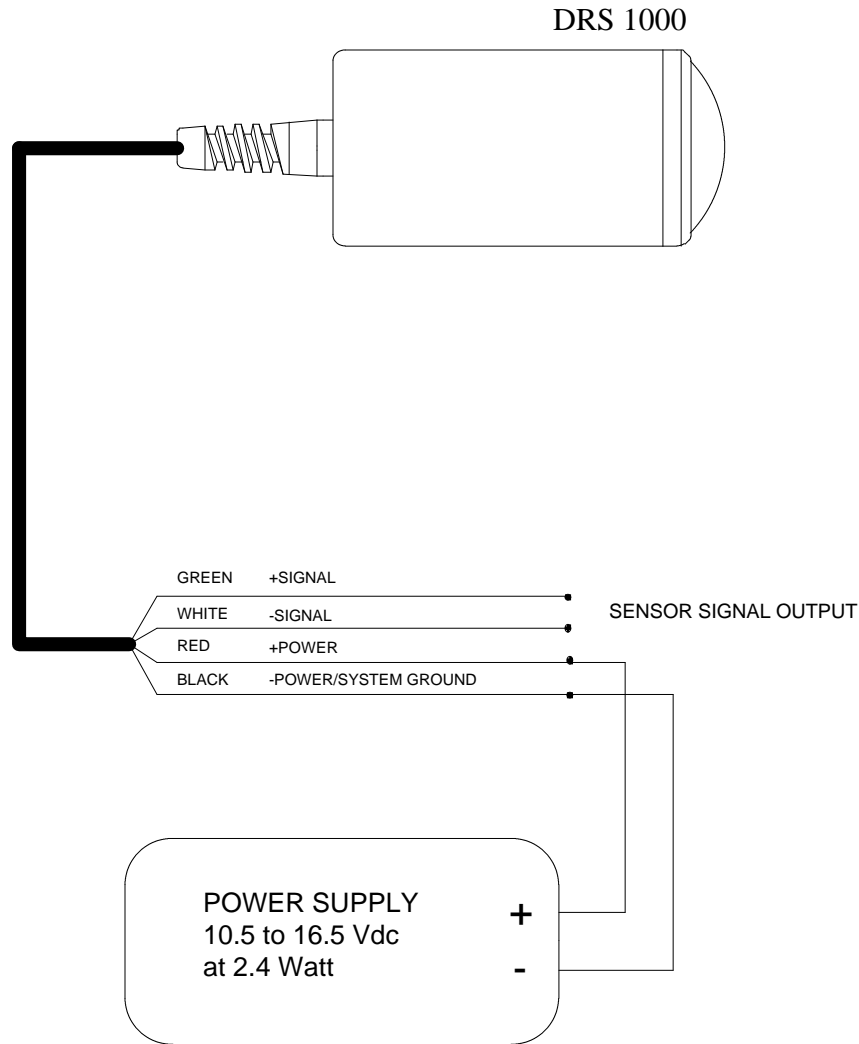


Figure 2 - Sensor Dimensions (not to scale)

Optional mounting brackets available

Information furnished by GMH Engineering is believed to be accurate & reliable. No responsibility is assumed, however, by GMH Engineering for its use, whether correct or incorrect; nor can GMH Engineering be held liable for consequences or any infringements of patents or other rights of third parties which may result from its use. Information in this document is current as of date of writing and is subject to change. Test data are representative of sensor performance under specific test conditions. Actual performance may vary with application and environment.

# DRS 1000 SIGNAL/POWER INTERFACE



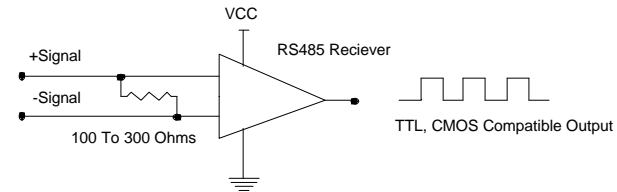
The signal output from the DRS1000 speed sensor is a 0 to 5 volt differential line driver that meets RS485 specifications. This type of output driver may be interfaced to the monitoring electronics in a number of ways. Three interfacing options are shown.

**OPTION 1. Fully Differential** - To maintain the integrity of the output signal over long distances (greater than 10 or 20 meters) or in electrically noisy environments, it is recommended that twisted pair wiring and an RS485 receiver with a line termination resistor be used. The termination resistor value will generally fall within a range of 100 to 300 ohms. This option is capable of maintaining the integrity of the sensor signal over many hundreds of meters of economical twisted pair cabling.

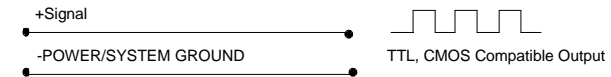
**OPTIONS 2 and 3. Single Ended** - For short transmission distances in relatively quiet electrical environments, the sensor output signal can be obtained by referencing either of the two differential outputs to the -POWER/SYSTEM GROUND node. The difference between Option 2 and Option 3 is a 180 degree phase shift between the two outputs. It is possible to monitor both of the differential outputs in this manner at the same time.

Under no circumstances should either of the differential outputs be grounded

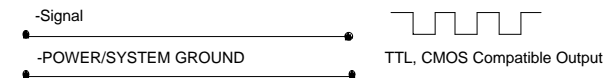
## SENSOR SIGNAL OUTPUT WIRING - OPTION 1



## SENSOR SIGNAL OUTPUT WIRING - OPTION 2



## SENSOR SIGNAL OUTPUT WIRING - OPTION 3



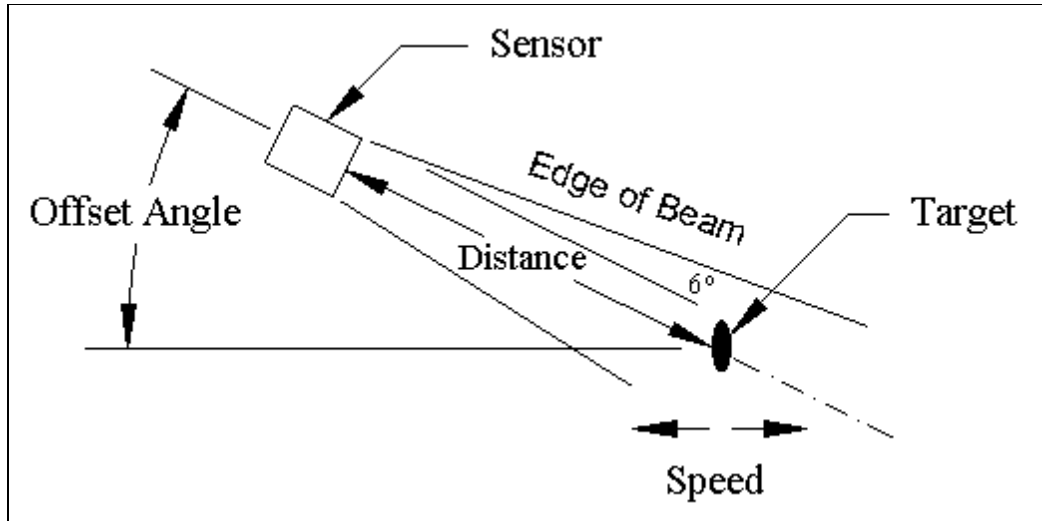


Figure 1 - Non Contact Speed Measurement

### Doppler Shift Frequency

Non-contact speed measurement using the Delta speed sensor is achieved through the use of Doppler Radar. Doppler radar is named after the Doppler principle, which explains the frequency shift associated with energy waves reflected by or emanated from a moving body. A familiar example of a Doppler shift is the change in pitch in the sound of a passing car - higher as the car approaches; lower as it leaves.

In the case of the Delta speed sensor, a Ka band radar signal is transmitted at a specific frequency by the sensor, reflects off of a target (or targets) and returns to the sensor (see Figure 1). If either the sensor or the target are moving relative to one another, the signal will be shifted in frequency when it returns to the sensor. This shift in frequency allows measurement of the relative velocity between the sensor and target.

The fundamental Doppler frequency shift is given by:  $F_d = 2 * V * (\frac{F_0}{c}) * \cos \theta$

where:  $F_d$  = Doppler Shift, Hz  
 $V$  = velocity  
 $\theta$  = offset angle of sensor relative to direction of target motion  
 $c$  = speed of light  
 $F_0 = 35.5 \pm 0.1$  GHz (Ka Band)

For the Delta speed sensor, the Doppler shift is  $105.799 \pm 0.298$  Hz / MPH (  $65.74074 \pm 0.185185$  Hz/KPH). The Delta speed sensor output is a square wave which is exactly twice the Doppler Shift, or  $211.598$  Hz / MPH ( $131.48148$  Hz/KPH).

### Correction for Offset Angle

As shown by the Doppler frequency shift equation, any offset angle (see Figure 1) between the center of the radar beam and target direction of travel will introduce a factor of cosine  $\theta$  into the measured speed. This means that the output of the sensor must be corrected by dividing into it the cosine of the offset angle as shown in this example:

case 1: Sensor Output: 5500 Hz      Offset Angle,  $\theta = 30^\circ$

$$\text{Actual velocity} = (5500\text{Hz} / (211.598\text{Hz/MPH})) / \cos 30^\circ = 30.01 \text{ MPH}$$

case 2: Sensor Output 5500 Hz      Offset Angle,  $\theta = 31^\circ$

$$\text{Actual velocity} = (5500\text{Hz} / (211.598\text{Hz/MPH})) / \cos 31^\circ = 30.32 \text{ MPH}$$

Also shown by this example, changes in offset angle can influence the speed measurement. For this reason it is recommended that the angle be known to at least  $1^\circ$ . This value will maintain an uncertainty of 1-2% for a target in the center of the beam. Because the value of cosine changes rapidly for angles above  $45^\circ$ , offset angles above  $45^\circ$  are not recommended

The radar beam diverges about  $6^\circ$  from center, resulting in a roughly conical-shaped beam. In the case of a target passing a fixed sensor, this geometry can introduce what is termed “cosine error” into the speed measurement. This happens because targets at one edge of the beam are at a different offset angle than in the center of the beam. For small offset angles, the cosine change from one edge of the beam to the other is small and so the cosine error is minimal. For larger offset angles, the change is more significant. In the case of vehicle ground speed measurements where the sensor is used to measure speed of a surface relative to the sensor, cosine error generally produces a steady bias. Refer to Application Note 1001 - Using Non-Contact Speed Sensing to Measure Vehicle Ground Speed for information.

### Signal Strength and Multiple Targets

The Delta speed sensor includes a signal processing algorithm that determines the strength of return signal from a target. If the signal is strong enough, the output is turned on and the sensor is said to be “locked”. Because different targets reflect different amounts of the radar energy back to the sensor, the sensor will lock at different distances from the target depending on such factors as target size, material and orientation.

In general, large targets reflect more energy and the sensor will be able to distinguish them at a greater distance. Highly reflective targets, such as metal will also reflect more energy than absorbent materials such as wood or plastic. If the target is a large flat, reflective surface, it will reflect a large amount of energy back to the sensor if it is oriented perpendicular to the beam, but much less if it is at an angle.

A useful analogy for deciding the amount of reflection in many cases is to think of the sensor as a flashlight. If the target surface would reflect a large amount of light back to the sensor, it is probable that it will return a strong signal. (Remember, however, that radar energy is at a different wavelength than visible light and the analogy will not work in all cases!)

The sensor receives reflected energy from all possible targets within the radar beam. If any of the targets are moving, it will cause a Doppler shift, possibly causing a false measurement if it is not the desired target. For this reason, it is important to consider the beam geometry, particularly the divergence angle, and make sure that the sensor cannot “see” non-targets.

### Contact Us

GMH Engineering personnel are available to discuss applications using the Delta Non-Contact Speed Sensor. If you have questions, please contact us at (801) 225-8970 or [info@gmheng.com](mailto:info@gmheng.com).

Information furnished by GMH Engineering is believed to be accurate & reliable. No responsibility is assumed, however, by GMH Engineering for its use, whether correct or incorrect; nor can GMH Engineering be held liable for consequences or any infringements of patents or other rights of third parties which may result from its use. Information in this document is current as of date of writing and is subject to change.
--

Rev. 1.0

# Application Note 1001

## Using Non-Contact Speed Sensing to Measure Vehicle Ground Speed

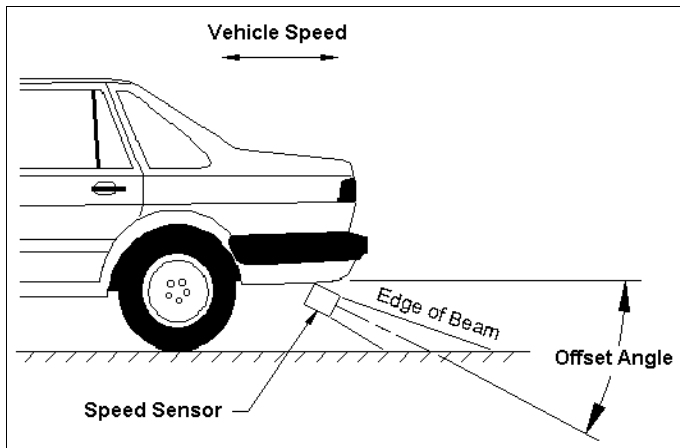


**Figure 1 - Measuring Vehicle Ground Speed (not to scale)**

Measuring vehicle ground speed is a straight-forward application of the non-contact speed sensor. As shown in Figure One, the sensor can be mounted on a vehicle, pointed at the ground and used to measure the speed of the vehicle relative to the ground. The sensor may be pointed either forward or backward.

An advantage of using a non-contact speed sensor over other methods such as measuring wheel rotation is that the speed measurement is not affected by factors like wheel slip, allowing a better measurement of true ground speed.

In one such measurement, the sensor was mounted pointing backward on a vehicle. The sensor was about one foot above the ground and was inclined downward from the horizontal by 30° (offset angle shown in Figure One). The sensor output was read by a counter channel on a GMH Engineering DataBRICK data acquisition system, which also applied a scale factor and corrected<sup>1</sup> for offset angle to produce the plot shown in Figure Two.

The data in Figure Two clearly show such features as gear shifting, acceleration, coasting and braking. In this test, the vehicle was driven over an asphalt surface, but the sensor may be used on other surfaces such as concrete, gravel or dirt.

### Offset Angle

The offset angle shown in Figure One is the *nominal* offset angle. This is the angle between the center axis of the radar beam and the horizontal in the vertical plane. Because of factors involving geometry and relative strengths of the return signal from areas on the ground ahead of and behind the center axis of the radar beam, the *effective* offset angle will differ from the nominal and requires a correction.

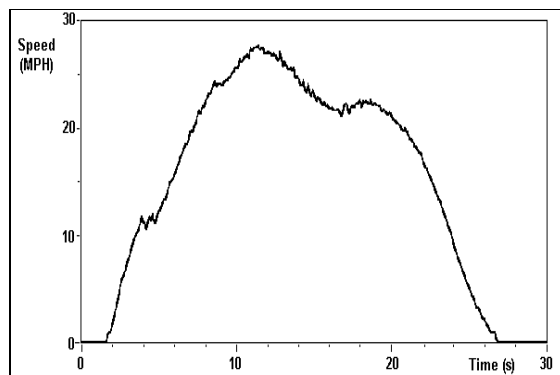


**Figure 2 - Vehicle Ground Speed (Miles per Hour)**

Table One shows the results of testing conducted to determine effective offset angles using the speed sensor on vehicles driven over asphalt. To use the table, replace the *nominal* offset angle actually used by the corresponding *effective* offset angle when correcting for offset angle<sup>1</sup>. For convenience, the cosine of the *effective* offset angle is also given in the table.

The particular choice of nominal offset angle involves a tradeoff between several factors. Placing the sensor at a steeper angle increases signal strength and reduces the field of view of the sensor so that it does not see non-targets, such as other vehicles. On the other hand, a steeper angle also increases sensitivity of the sensor to vertical motions and may introduce more variation in the vehicle ground speed measurement because of pitching of the vehicle on its suspension. For most applications involved in road testing, GMH Engineering uses a 30° nominal offset angle.

The accuracy of the speed measurement using this method of offset angle correction depends on the accuracy to which the offset angle is known. For instance, with a 30° offset angle, a 1° uncertainty in offset angle can cause a 1-2% uncertainty in the speed measurement. If greater accuracy is required the sensor can be calibrated by other methods, such as a distance comparison achieved by recording the number of pulses received from the sensor while the vehicle travels over a fixed distance.

**Table One - Effective Offset Angles On Asphalt**

Nominal Offset Angle (degrees)	Effective Offset Angle (degrees)	Cosine Effective Offset Angle	Nominal Offset Angle (degrees)	Effective Offset Angle (degrees)	Cosine Effective Offset Angle
20	24.12	0.9127	33	34.47	0.8245
21	24.82	0.9076	34	35.34	0.8157
22	25.54	0.9023	35	36.22	0.8068
23	26.28	0.8966	36	37.11	0.7975
24	27.04	0.8907	37	38.00	0.7880
25	27.82	0.8844	38	38.90	0.7782
26	28.61	0.8779	39	39.80	0.7682
27	29.41	0.8711	40	40.71	0.7580
28	30.23	0.8640	41	41.63	0.7475
29	31.05	0.8567	42	42.54	0.7368
30	31.89	0.8490	43	43.47	0.7258
31	32.74	0.8411	44	44.39	0.7146
32	33.60	0.8329	45	45.32	0.7031

**Other Considerations**

The sensor should be aligned parallel to the direction of vehicle travel so that there is no horizontal offset angle. It is also important to consider factors such as suspension pitching, vibration, dust or water spray when choosing a mounting location for the sensor. For example, a forward-pointing sensor may be indicated for applications where dust or water spray is expected at the rear of the vehicle which might interfere with the radar beam. The sensor should be mounted on a rigid location located away from engine vibration. Some suspension pitching is evident in Figure Two, where the vehicle under test was, in fact, driven over bumps and had a stiff suspension. These effects could be removed, if desired, by post-processing to smooth the data. If these factors are taken into consideration measurements of vehicle ground speed can be made for a wide variety of applications.

**Contact Us**

GMH Engineering personnel are available to discuss applications using non-contact speed sensing. If you have questions, please contact us at (801) 225-8970 or info@gmheng.com.

<sup>1</sup> see *Application Note 1000 Fundamentals of Non-Contact Speed Measurement Using Doppler Radar*

Information furnished by GMH Engineering is believed to be accurate & reliable. No responsibility is assumed, however, by GMH Engineering for its use, whether correct or incorrect; nor can GMH Engineering be held liable for consequences or any infringements of patents or other rights of third parties which may result from its use. Information in this document is current as of date of writing and is subject to change.

APPENDIX D

COST BENEFIT ANALYSIS

It is known that job-related neck, shoulder, and low-back injuries rank first in cost to worker's compensation insurance claims in many countries (Cunningham and Kelsey<sup>4</sup>). It is also known that prolonged inclinations of the head and trunk, as shown by the striper operator in figure 2, are work-related risk factors for on-the-job injuries. It has been shown<sup>5</sup> that there is a relationship between job-related non-neutral trunk bending of more than 20° and musculoskeletal disorders and that neck and shoulder disorders are related to the time spent with the neck in flexion and twisted, all of which are common to the operator's posture shown in figure 2.

Of the 16 maintenance activities under which the Caltrans Office of Safety and Health categorizes injury and motor vehicle costs, traffic guidance (which includes striping) ranks 3<sup>rd</sup> in annual costs over the last decade. The Caltrans Office of Safety and Health reports<sup>6</sup> that the annual cost of injuries associated with striping was \$68,604 and the annual cost of motor vehicle accidents associated with striping was \$29,600 over the last 10.5 years. Personal communication with experienced striper operators indicates that the boom mounted mirror used in striper guidance presents a significant safety risk when an occasional California driver exercises poor judgement in attempting to pass the striper during operation and risks the safety of everyone involved when they collide with the mirror.

According to a study done by Hashemi et al.<sup>7</sup> work-related musculoskeletal disorders of the upper extremity had a 1994 median cost per injury of \$500 and resulted in a median number of days lost from work of 5 per injury. Thus with \$68,604 in annual injury costs per year associated with striping there would be a corresponding 686 ( $5 * \$68,604 / \$500 = 686$ ) lost person days of work due to injury. On the average, striping requires 58.23 person years of labor each year. Dividing the total labor cost by the number of person years and assuming 250 work days per year the labor cost is about \$183.75 for each person day ( $\$2,674,940 / (58.23 * 250) = \$183.75$ ). Thus we can estimate the annual median cost due to lost days of work (these are in addition to the direct injury costs reported by the Office of Safety and Health) associated with injuries to be \$126,053 ( $686 \text{ lost person days} * \$183.75 \text{ per person day} = \$126,053$ ).

The total annual cost associated with injuries, motor vehicle accidents, lost days work and labor is estimated at \$2,899,196. Automation of the striping task should reduce these costs. In

---

<sup>4</sup> Cunningham, L.S. and J.L Kelsey. 1984. Epidemiology of musculoskeletal impairments and associated disability. *Am. J. of Public Health.* 74:574-579.

<sup>5</sup> Van Riel, M.P.J.M., J.C.M Derksen, A. Burdorf, and C.J. Snijders. 1995. Simultaneous measurements of posture and movements of head and trunk by continuous three-dimensional registration. *Ergonomics* 38(12):2563-2575.

<sup>6</sup> Caltrans Office of Safety and Health. Caltrans maintenance program injury and motor vehicle accident costs by maintenance activity (1/1/90-7/1/00).

<sup>7</sup> Hashemi, L., B.S. Webster, E.A. Clancy, and T.K. Courtney. 1998. Length of disability and cost of work-related musculoskeletal disorders of the upper extremity. *JOEM* 40(3):261-269.

addition to these benefits which are readily quantified in economic terms, there are benefits to California drivers associated with more accurately striped lanes and to Caltrans in the ability to better utilize less experienced operators in the striping task, which are more difficult to assess in specific dollar amounts.

## APPENDIX E

### CD-ROM MOVIE OF ZICAM OPERATION

An AVI-type movie file named “zicam\_movie.avi” can be found on this CD-ROM. For best results, copy the file to your computer’s hard disk and play the movie using a software package such as Windows Media Player (available from [www.microsoft.com](http://www.microsoft.com)) or Quicktime Player (available from [www.apple.com](http://www.apple.com)).